Universidade de Aveiro
2013

Departamento de Electrónica, Telecomunicações e Informática

José Eduardo Leal Moreira

Esquemas de pré-codificação IA com IB-DFE para sistemas MC-CDMA

IB-DFE with interference alignment precoding scheme for MC-CDMA systems

Universidade de Aveiro
2013

Departamento de Electrónica, Telecomunicações e Informática

José Eduardo Leal Moreira

Esquemas de pré-codificação IA com IB-DFE para sistemas MC-CDMA

IB-DFE with interference alignment precoding scheme for MC-CDMA systems

Dissertação apresentada à Universidade de Aveiro para cumprimento dos requisitos necessários à obtenção do grau de Mestre em Engenharia Electrónica e Telecomunicações, realizada sob a orientação científica do Prof. Dr. Adão Paulo Soares da Silva do Departamento de Electrónica, Telecomunicações e Informática da Universidade de Aveiro e do Prof. Dr. Atílio Manuel da Silva Gameiro do Departamento de Electrónica, Telecomunicações e Informática da Universidade de Aveiro.

o júri

presidente / president

Prof. Dr. Arnaldo Silva Rodrigues de Oliveira
Professor Auxiliar do Departamento de Electrónica, Telecomunicações e Informática da Universidade de Aveiro

orientador / adviser

Prof. Dr. Adão Paulo Soares da Silva
Professor Auxiliar do Departamento de Electrónica, Telecomunicações e Informática da Universidade de Aveiro

arguente / examiner

Prof. Dr. Carlos Miguel Nogueira Gaspar Ribeiro
Professor Adjunto do Departamento de Engenharia Electrotécnica da Escola Superior de Tecnologia e Gestão do Instituto Politénico de Leiria

agradecimentos Agradeço a todos os que me acompanharam neste percurso.

palavras-chave OFDM, MC-CDMA, IA, MIMO, ZF, MMSE, IB-DFE

resumo

Para atingir maiores ritmos de transmissão, as futures aplicações multimédia necessitam de atingir a qualidade de serviço necessária. Para isso, o *multi-carrier code division multiple access* (MC-CDMA) tem sido apontado como um forte candidato para interface ar dos futuros sistemas celulares. O *Interference Alignment* (IA) ou alinhamento de interferência é uma técnica promissora que permite ter altos ganhos de capacidade em canais com interferência. Por outro lado, temos receptores baseados no conceito *iterative block decision feedback equalization*(IB-DFE) que conseguem tirar partido, de uma forma eficiente, da inerente diversidade espaço-frequência dos sistemas MIMO MC-CDMA.

Nesta dissertação é implementada uma pré-codificação baseada no conceito de IA considerando três transmissores (ou estações base) juntamente, com um processamento IB-DFE no receptor para sistemas MC-CDMA.A pré-codificação é aplicada ao nível de chip em vez de ser aplicado ao nível dos dados. O receptor é projectado em dois passos: em primeiro lugar equalizadores baseados em ZF ou em MMSE são utilizados para remover a interferência alinhada dos restantes utilizadores. De seguida, e após aplicar um processo de branqueamento do ruído ao sinal à saída do primeiro equalizador, um segundo equalizador baseado em IB-DFE é projectado para remover a interferência inter-utilizador residual e também a interferência residual entre portadoras.

Os resultados obtidos mostraram-se satisfatórios na remoção da interferência obtendo-se um desempenho muito próximo do obtido considerando um filtro adaptado.

keywords OFDM, MC-CDMA, IA, MIMO, ZF, MMSE, IB-DFE

abstract

To achieve high bit rates, needed to meet the quality of service requirements of future multimedia applications, multi-carrier code division multiple access (MC-CDMA) has been considered as a candidate air-interface. Interference alignment (IA) is a promising technique that allows high capacity gains in interfering channels. On the other hand, iterative block decision feedback equalization (IB-DFE) based receivers can efficiently exploit the inherent space-frequency diversity of the MIMO MC-CDMA systems.

In this thesis we proposed an IA precoding at the transmitter with IB-DFE based processing at the receiver for MC-CDMA systems. The IA precoding is applied at chip level instead of the data symbols level, as in the conventional IA based systems. The receiver is designed in two steps: first the equalizers based on zero forcing (ZF) or minimum mean square error (MMSE) are used to remove the aligned users´ interference. Then and after a whitening noise process, an IB-DFE based equalizer is designed to remove both the residual inter-user aligned and inter-carrier interferences.

The results have shown that the obtained performance is very close to the one obtained by the optimal matched filter, with few iterations at the receiver side.

Contents

List of Figures

List of Tables

Acronyms

AMPS	Advanced Mobile Phone System
BER	Bit Error Rate
BS	Base Station
CDMA	Code Division Multiple Access
DFE	Decision Feedback Equalization
DFT	Discrete Fourier Transform
EDGE	Enhanced Data for GSM Evolution
FDE	Frequency Domain Equalization
FFT	Fast Fourier Transform
GPRS	General packet radio service
GSM	Global System for Mobile Communications
HSDPA	High Speed Downlink Packet Access
HSPA	High Speed Packet Access
HSUPA	High Speed Uplink Packet Access
IA	Interference Alignment
IB	Iterative Block
IB-DFE	Iterative Block Decision Feedback Equalization
ICI	Inter Carrier Interference
IDFT	Inverse Discrete Fourier Transform
IEEE	Institute of Electrical and Electronics Engineers
IFFT	Inverse Fast Fourier Transform
ISI	Inter Symbol Interference
LTE	Long Term Evolution
MAI	Multiple Access Interference
MC	Multi Carrier
MF	Match Filter
MIMO	Multi Input Multi Output
MISO	Multi Input Single Output

MMSE	Minimum Mean Square Error
OFDM	Orthogonal Frequency Division Multiplex
OFDMA	Orthogonal Frequency Division Multiple Access
PAPR	Peak Average Power Ratio
PIC	Parallel Interference Cancelation
QPSK	Quaternary Phase Shift Keying
SC	Single Carrier
SC-FDE	Single Carrier with Frequency Domain Equalization
SIMO	Single Input Multiple Output
SINR	Signal to Interference plus Noise Ratio
SISO	Single Input Single Output
SNR	Signal to Noise Ratio
UE	User Equipment
UMTS	Universal Mobile Telecommunications System
WCDMA	Wideband Code Division Multiple Access
WiMAX	Worldwide interoperability for Microwave Access
ZF	Zero Forcing

1. Introduction

1.1. Evolution of Cellular Systems

The initial mobile networks of the mid-1980s, referred to as 1G network, were based on analogue communication. These types of networks had a limited regional scope, which was mostly confined to national boundaries. In the early 1990s, there was a replacement of these analogue networks with the digital second generation (2G) networks. The technology which emerged with more potential and became more popular was the Global System for Mobile communications (GSM) between the 2G standards and it is believed there are more than 6 billion of subscribers[1] as shown in Fig. 1.1.

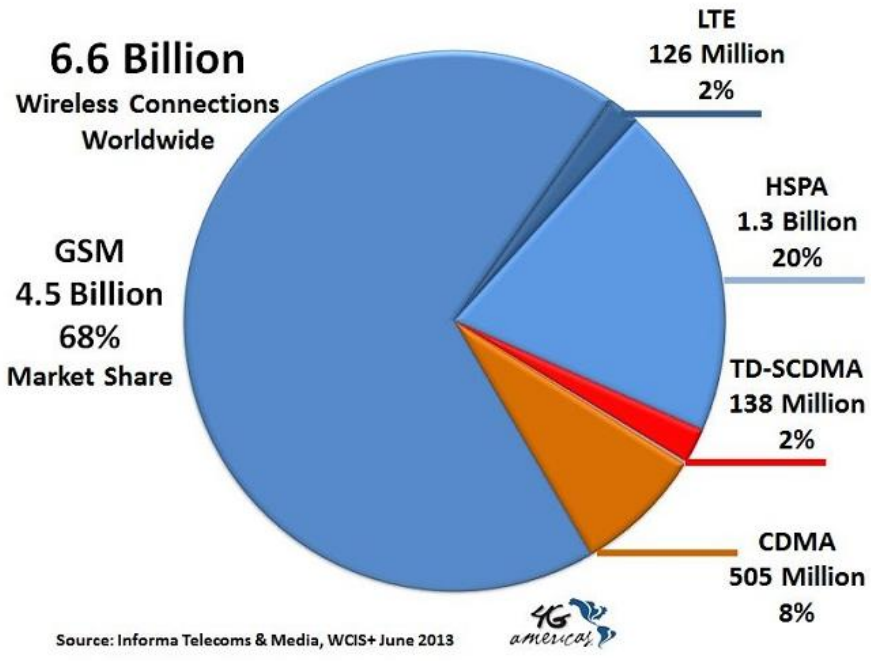

Fig. 1.1 Mobile market shares by technology.

The success of 2G technologies provided the needed thrust to mobile wireless communications and opened the doors for the enhanced networks which appeared in the future. There were two big differences that marked the shift from 1G and 2G. Firstly, 2G was based on digital communication, both in the radio path and between network entities and secondly, the processes implemented for 2G standards were aimed to make the notion of global roaming more realistic. The following four different 2G technologies are in use:

GSM used 25 MHz frequency spectrum in the 900 MHz band divided into 124 carrier frequencies of 200 kHz each. A single 200 kHz radio channel was shared between eight users by allocating a unique time slot to each one of them. GSM is a combination of two multiplexing techniques, namely, Frequency Division Multiple Access (FDMA) and Time Division Multiple Access (TDMA)[2].

Another technology used is the Interim Standard-95 (IS-95) that used another scheme of multiplexing called Code Division Multiple Access (CDMA). This scheme use different codes to distinguish data between different users on the same frequency. It was popular in South Korea and United States and offered tough competition to GSM.

In Japan, the 2G technology Personal Digital Communications (PDC) obtained immense popularity, however it was not very popular amongst other countries.

In North America emerged another technology known as US-TDMA or D-AMPS (Digital – Advanced Mobile Phone Services). This technology is backward-compatible with AMPS and it is the digital version of the 1G system AMPS.

The limitations observed on 2G technologies brought up another type of networks known as 2.5G. These networks came to end up the limitations in 2G like the low transfer rates since 2G networks were, primarily, designed to offer voice services; the low efficiency for packet-switched services once the 2G networks were not prepared to access Internet efficiently; multiple standards which allows a limited roaming since users only can roam into networks which support the same standard. The outcomes to deal with these limitations were the 2.5G networks where the main objective was to make minimum changes in the existing network architecture. The different categories of 2.5G networks are:

High-Speed Circuit-Switched Data (HSCSD) uses multiple time slots instead of one, i.e., increases the data rate by the number of time slots.

General Packet Radio Services (GPRS) offers data services by using packet-switching domain. GPRS uses 1 to 8 radio channels to offer speeds of up to 115 kbps. GPRS is an important advantage because provides the means to migrate to 3G networks and the core network components of GPRS are an integral part of 3G core network[3].

Enhanced Data Rates for Global Evolution (EDGE) could increase the data rates of GSM and GPRS up to three times by using better modulation techniques. This improvement is called EDGE for GSM and Enhanced GPRS (EGPRS) for GPRS where a speed of up to 384 kbps can be obtained[4].

The third generation was introduced to satisfy the demand for higher bandwidth by the International Telecommunication Union (ITU) known as International Mobile Telecommunications-2000 (IMT-2000) at the time. The dominant 3G technology in the world is Universal Mobile Telecommunication System (UMTS). UMTS was developed from GSM by changing the air interface but keeping the core network almost unchanged. The UMTS air interface had two different implementations: the Wideband code division multiple access (WCDMA) and the time division synchronous code division multiple access (TD-SCDMA) which was developed in China. The main differences between these 3G technologies are: WCDMA segregates the base stations' and mobiles' transmissions in frequency division multiplex and a bandwidth of 5 MHz while TD-SCDMA uses time division multiplex in a bandwidth of 1.6 MHz.

At the same period, CDMA2000 was developed from IS-95 and is mainly used in North America and both specifications, IS-95 and CDMA2000, were produced by the Third Generation Partnership Project 2 (3GPP2). CDMA2000 uses a bandwidth of 1.25MHz, it is backwards compatible with IS-95 and it separates the voice traffic and optimized data onto different carrier frequencies. Due to fact that North America market presents a large number of IS-95 devices and few available 5 MHz bands difficult the penetration of UMTS technology into North America[5].

These, UMTS and CDMA2000, systems were later enhanced for data applications. UMTS was upgraded into High Speed Packet Access (HSPA) which is the combination of High

Speed Downlink Packet Access (HSDPA) on Release 5 with High Speed Uplink (HSUPA) on Release 6 that offered speed up to 14.4 Mbps downlink and 5.76 Mbps uplink using the same frequency bands. HSPA+ also referred to as HSPA Evolved is a further 3GPP enhancement to HSPA Rel-6. HSPA+ and provides an increase in both downlink and uplink modulation efficiency as well as support for (2x2) Multi Input Multi Output (MIMO) at the base station. HSPA 3GPP Rel-7 supports 64QAM in the downlink and 16QAM in the uplink. Rel-7 also provides support for (2x2) MIMO in the downlink. Since HSPA+ enhancements are backwards compatible with 3GPP Rel-5 and 3GPP Rel-6 it represents a relatively straightforward migration path for WCDMA operators to increase key performance attributes in the access network.

CDMA2000 was upgraded to CDMA2000 Evolved-Data Optimized (EV-DO Rev 0) which allows data rates of 2.4 Mbps downlink and 153 kbps uplink. The revision A allows data rates of 3.1 Mbps downlink and 1.8 Mbps uplink as also Orthogonal Frequency Division Multiplex (OFDM) waveform has been introduced into Revision A to offer high capacity multicast capabilities that will allow service providers to offer lower cost multicast services while maintaining a robust high speed mobile network[6].

In 1999, the Institute of Electrical and Electronics Engineers (IEEE) Standards Board established the IEEE 802.16 Working Group on Wireless Standards (also known as IEEE 802 LAN/MAN Committee), which aims to prepare formal specifications for the deployment of Wireless Metropolitan Area Networks (WMAN) around the world. This family of standards is officially named WirelessMAN, but was later changed to Worldwide Interoperability for Microwave Access (WiMAX) by an industry group called the WiMAX Forum, with a mission to certify and promote interoperability and compatibility of wireless products. On the other hand, Mobile WiMAX takes a fixed application a step further to allow any telecommunication to go mobile. Though considered as more complex, this enables handsets, data devices and mobile phones on a much larger scale. Such technology must support a wireless connection from a base station to another while the subscriber is moving, without any interruption. This standard was completed in December of 2005. The Mobile WiMAX Air Interface adopts Orthogonal Frequency

Division Multiple Access (OFDMA) for improved multi-path performance in non-line-of-sight environments. The main features of WiMAX are the inclusion of MIMO with Advanced Coding and Modulation to support peak downlink data rates up to 63 Mbps and up to 28 Mbps, Quality of Service (QoS), scalability since it is designed to work in different channelization from 1.25 MHz to 20 MHz, improved security with Extensible Authentication Protocol (EAP) based authentication, AES-CCM based authenticated encryption and Cipher-based Message Authentication Code (CMAC) and Hashed Message Authentication Code (HMAC) based control message as well as an optimized handover schemes with latencies less than 50 milliseconds to ensure real-time applications to improve mobility[7].

Long term evolution (LTE) was the next step forward in cellular 3G services. LTE technology is based on a 3GPP standard that provides for a downlink speed of up to 150 megabits per second (Mbps) and an uplink speed of up to 50 Mbps. Fixed wireless and wired standards are already approaching or achieving 100 Mbps or faster, and LTE is a way for cellular communications to operate at that high data rate.

The LTE standard grew out of the Global System for Mobile Communications (GSM) and Universal Mobile Telecommunications System (UMTS) standards, commonly called 3G. Voice communication was the primary application, with data added recently. Mobility and seamless handoff were requirements from the start, as was a requirement for central management of all nodes. LTE speeds will be equivalent to what today's user might see at home on a fast cable modem. The LTE standard is designed to enable 150 Mbps downlink and 50 Mbps uplink over a wide area. While 150 Mbps is LTE's theoretical top uplink speed, each user's bandwidth will depend on how carriers deploy their network and available bandwidth. The LTE physical layer is unique because it has asymmetrical modulation and data rates for uplink and downlink. The standard is designed for full-duplex operation, with simultaneous transmission and reception. The radio is optimized for performance on the downlink, because the transmitter at the base station has plenty of power. On the uplink, the radio is optimized more for power consumption than

efficiency, because while processing power has increased, mobile device battery power has stayed essentially constant. LTE uses as downlink multiple access the OFDMA and onto uplink the Single Carrier Frequency Division Multiple Access (SC-FDMA). This new air technique, SC-FDMA, was developed because it combines the advantages of multicarrier technologies with the advantages of the single carrier technologies such as the multipath resistance presented by the OFDM with the low Peak-to-Average Power Ratio (PAPR) from the single carrier formats[8]. The LTE was designed to meet the following goals[9]:

1. Support scalable bandwidths
    - 1.25, 2.5, 5.0, 10.0 and 20.0 MHz
2. Peak data rate that scales with system bandwidth
    - Downlink (2 Channel MIMO) peak rate of 100 Mbps in 20 MHz channel
    - Uplink (single Channel Transmission) peak rate of 50 Mbps in 20 MHz channel
3. Supported antenna configurations
    - Downlink: 4x2, 2x2, 1x2, 1x1
    - Uplink: 1x2, 1x1
4. Spectrum efficiency
    - Downlink: 3 to 4 x HSDPA Rel. 6
    - Uplink: 2 to 3 x HSUPA Rel. 6
5. Latency
    - Control-plane: <50 – 100 ms to establish User-plane
    - User-plane: <10 ms from UE to server
6. Mobility
    - Optimized for low speeds (<15 Km/h)
    - High performance at speeds up to 120 Km/h
    - Maintain link at speeds up to 350 Km/h
7. Coverage
    - Full performance up to 5 Km
    - Slight degradation 5 km – 30 Km
    - Operation up to 100 Km should not be precluded by standard

It is expected that the number of LTE subscribers increase exponentially in the near future as described in Fig. 1.2.

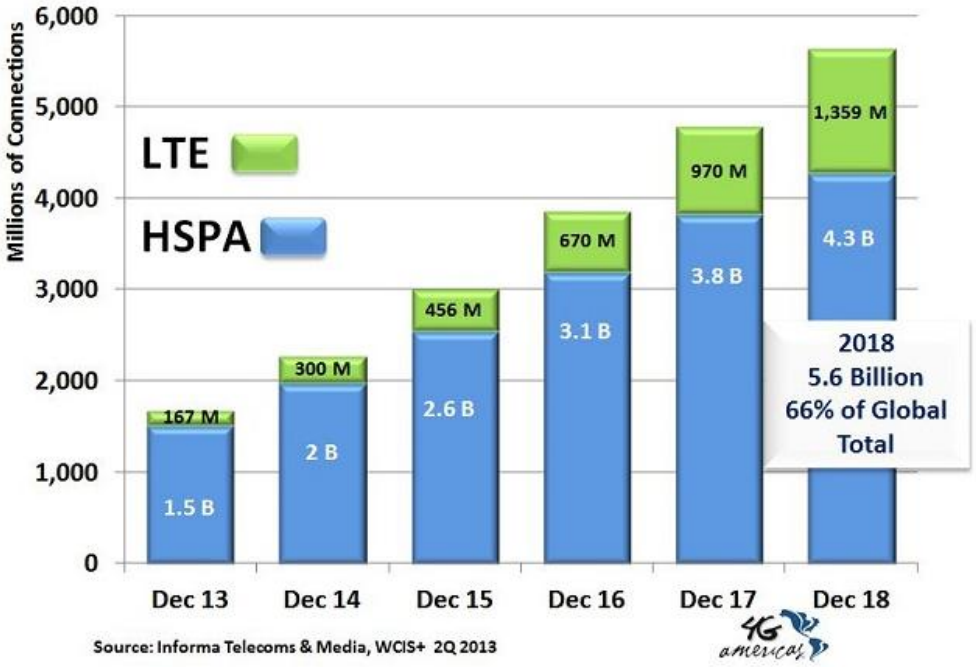

Fig. 1.2 Estimation of Future Subscriptions of LTE[10].

1.2. Multicarrier Systems Concept

1.2.1. Orthogonal Frequency Division Multiplex

OFDM was firstly proposed in 1968 and patented in 1970. The first application using this technique in mobile communications was presented in 1985[11].

OFDM technique emerged as an evolution of FDM (Frequency Division Multiplex) where, instead of having guard bands separating the subcarriers, we have several subcarriers spectrally overlapped. OFDM communication systems do not rely on increased symbol rates to achieve higher data rates like its predecessors single carrier systems.

The principle of OFDM consists in breaking the available bandwidth into many orthogonal narrower sub-carriers and transmitting the data in parallel streams. By dividing the bandwidth in narrower bands reduces the data rate which increases the duration of the symbol in each sub-carrier and provides a decrease of the sensitivity and frequency selectivity caused by multipath distortion. Besides, the OFDM technique uses a cyclic prefix to be more efficient to this type of fading.

OFDM brings, as an important benefit, the possibility to work in frequency domain which allows easier signal improvement techniques comparatively the same techniques in the time domain.

1.2.2. Multicarrier Code Division Multiple Access

Multicarrier code division multiple access (MC-CDMA) was firstly proposed in 1993 and completely outlined in 1997.This scheme combines efficiently OFDM and code division multiple access (CDMA). Therefore, MC-CDMA benefits from OFDM characteristics such as high spectral efficiency and robustness against multi-path propagation, while CDMA allows a flexible multiple access with good interference properties for cellular environments[12][13].

In MC-CDMA based systems, the different users share the same bandwidth at the same time and the data is separated by applying different user specific spreading codes, i.e., users are separated in the code domain. As in the OFDM, The multicarrier symbol duration is higher than the single carrier one and thus the ISI is reduced.

The principle of MC-CDMA is to map the chips of a spread data symbols in frequency direction over several parallel sub-channels, i.e., each chip of the direct sequence is mapped onto a different sub-carrier.

MC-CDMA provides good probability-of-error performance in frequency selective fading channels. However, MC-CDMA experiences performance degradation due to Multi Access Interference (MAI) caused by the others active users that are sharing the same carriers. MC-CDMA system performance is limited by the presence of this type of interference[14].

1.3. Interference Alignment Concept

Analysis of interference channels has shown that capacity of an interference channel for a given user is one half the rate of its interference-free capacity in the high transmit power regime, for any number of users[15]. One interesting recent scheme to efficiently eliminate the interference and achieve a linear capacity scaling is interference alignment (IA).

In a relatively short time, this concept has challenged much of the conventional wisdom about the throughput limits of both wired and wireless networks. A representative example is the wireless interference channel with *K* transmitter–receiver pairs where, because of interference alignment, each user is simultaneously able to send at a data rate equal to half of his interference-free channel capacity to his desired receiver, even though the number of users *K* can be arbitrarily large, thus showing that the interference channel is not fundamentally interference limited.

This recently used technique allows the transmitters to align in the unwanted users' receive signals in any dimension, through the use of precoders. With this strategy more interferers can be completely cancelled than with other interference cancellation methods, thus achieving the maximum degrees of freedom[16]. Applications of IA include cellular networks, two-way communication networks, cooperative communication networks, cognitive radio networks, etc[17].

1.4. Motivations and objectives

The increasing demand for wireless services has created the need for cost effective transmission techniques that can exploit scarce spectral resources efficiently. To achieve high bit rates, needed to meet the quality of service requirements of future multimedia applications, MC-CDMA has been considered as a air-interface candidate, especially for downlink[18]. However, the user capacity of MC-CDMA system is essentially limited by interference. This interference can be mitigated by employing precoding techniques[19],

and/or iterative block decision feedback equalization (IB-DFE) based receivers[20]. Conventional frequency domain equalization (FDE) schemes usually employ a linear FDE optimized under the minimum mean square error (MMSE) criterion. However, the residual interference levels might be too high, leading to performance that is still several dB from the matched filter bound (MFB).

As discussed, IA is a promising technique that allows high capacity gains in interfering channels. On the other hand, iterative frequency-domain detection receivers based on the IB-DFE concept can efficiently exploit the inherent space-frequency diversity of the MIMO MC-CDMA systems. Therefore, in this thesis we consider IA precoding at the transmitter with IB-DFE at the receiver for MIMO MC-CDMA systems. To the best of our knowledge joint IA-precoding and IB-DFE for MC-CDMA systems has not been addressed in the literature. In the proposed scheme the chips are IA-precoded instead of the data symbols as in the narrowband or OFDM systems. The receiver is designed in two steps: first a standard MMSE equalizer is used to mitigate the aligned users´ interference, then and after a whitening noise process, an IB-DFE based equalizer is designed to mitigate both the residual inter-user and inter-carrier interferences. Our proposed scheme achieves the maximum degrees of freedom, while allowing a close-to-optimum diversity gain, with only a few iterations at the receiver side.

1.5. Contributions

The main results of this thesis have been published in

Adão Silva, José Moreira, Rui Dinis, and Atílio Gameiro, "Joint Interference Alignment and IB-DFE scheme for MC-CDMA Systems ", in. Proc. International Conf. on Signal Processing and Communication Systems (ICSPCS), Gold Coast, Australia, Dec. 2013.

1.6. Outline

After the presentation of the evolution of the cellular systems and the basic concepts of OFDM, MC-CDMA and IA and the main objectives of this thesis we will continue with the following chapters:

In chapter 2 it is presented the multicarrier systems as OFDM and MC-CDMA. It will be presented the definition of OFDM and MC-CDMA and the combination of them. The study was focused in the downlink and blocks diagrams are presented for their transmitters and receivers.

In Chapter 3, it will be introduced the systems and techniques, which we work to be able to develop the system presented later, like MIMO techniques, the iterative block equalizer and a deeper view about Interference Alignment as the specific and closed case of three users free from interference.

In Chapter 4, it is developed the system that has been implemented which is the core of this thesis. It will be presented the how the technologies referred in the other chapters were combined and the outcome that the implemented system has produced.

For the last, in Chapter 5 the thesis is concluded and a brief summary of the developed system and future work will be given.

2. Multicarrier Systems

The principle of multicarrier-transmission is to convert a serial high-rate data stream onto multiple parallel low-rate sub-streams where each sub-stream is modulated on another sub-carrier. Since the symbol rate on each sub-carrier is much less than the initial serial data symbol rate, the effects of ISI is significantly decreased, reducing the complexity of the equalizer. In this chapter, it is given an overview of two multicarrier systems, namely, OFDM and MC-CDMA.

2.1. Orthogonal Frequency Division Multiplex

As briefly described in chapter 1, OFDM divides the available bandwidth into many orthogonal sub-carriers that there are carefully selected in a way to be orthogonal between each other, i.e., when we have a maximum in a sub-carrier, the others have a passage to zero, as shown in Fig 2.1.

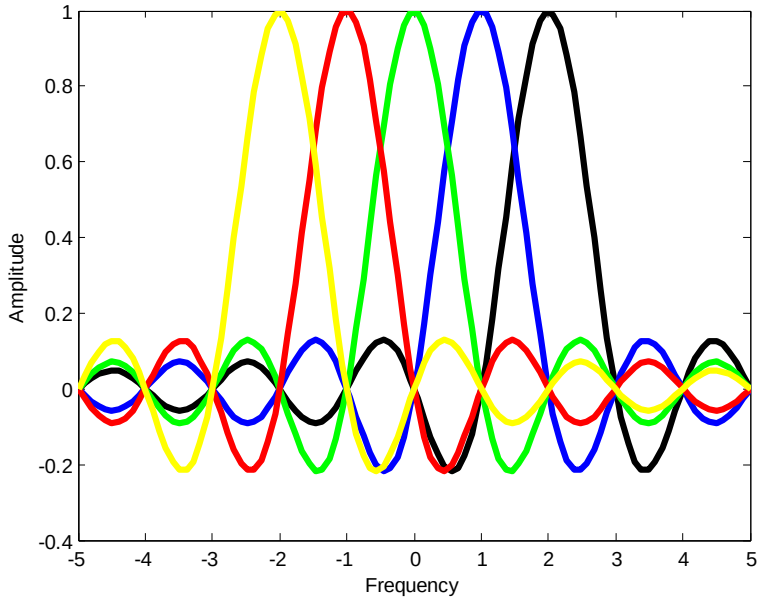

Fig. 2.1 Sub-carriers normalized in an OFDM system.

In Fig. 2.2 we can see a block diagram multi-carrier modulator employing OFDM.

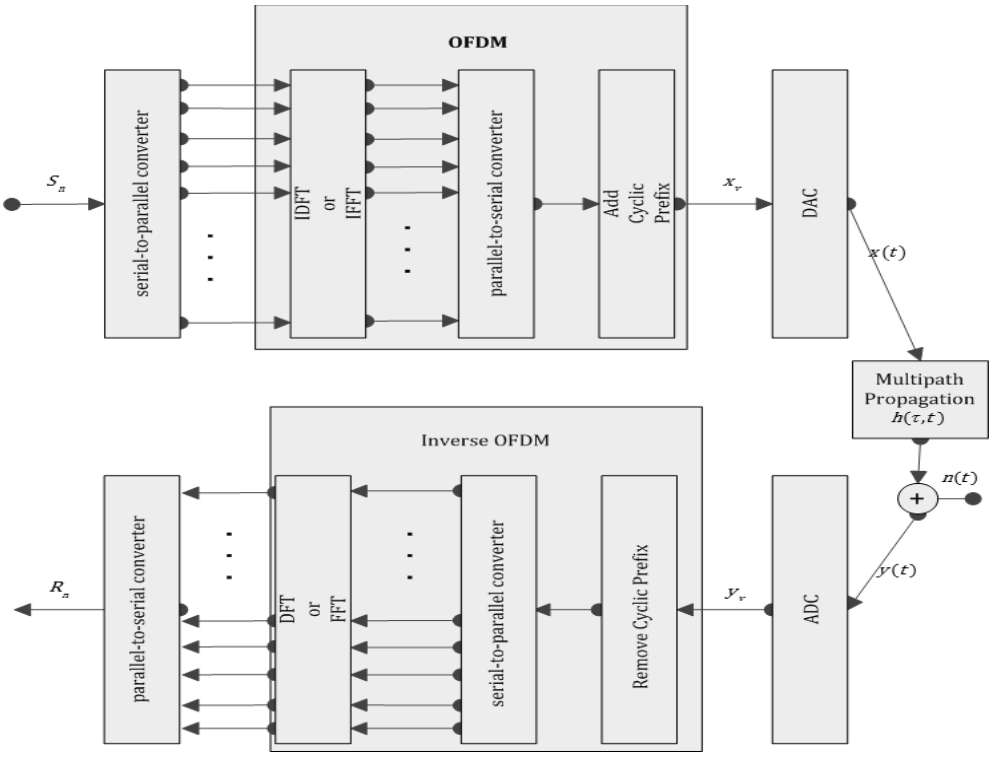

Fig. 2.2 Digital multi-carrier transmission system applying OFDM.

A communication system with multi-carrier modulation transmits N_c complex-valued symbols S_n,n=0…, $N_c - 1$, in parallel N_c sub-carriers. The source symbol duration T_d results after serial-to-parallel conversion in the OFDM symbol duration

$$T_s = N_c T_d \tag{2.1}$$

OFDM modulate the N_c sub-streams on sub-carriers with spacing of

$$F_s = \frac{1}{T_s} \tag{2.2}$$

In order to achieve orthogonality between the sub-carriers. The OFDM symbol is referred as the N_c parallel modulated symbols S_n,*n*=0…, $N_c - 1$.

Although there are modulated sub-carriers spectrally overlapped, each sub-carriers data can be isolated from the others through an adequate filter. However, to verify this orthogonality, it is necessary sub-carriers to be centred with respective frequencies of OFDM sub-channels and the due clock synchronization. This spectral overlap produces a significant band economy comparatively to the FDM traditional technique which is approximately 50%.

The complex envelope of an OFDM symbol is

$$x(t) = \frac{1}{N_c} \sum_{n=0}^{N_c} S_n e^{j2\pi f_n t}, 0 \le t \le T_s \tag{2.3}$$

where the N_c sub-carrier frequencies are located at

$$f_n = \frac{n}{T_s}, n = 0, \ldots, N_c \tag{2.4}$$

The generation of OFDM signal would require a larger number of coherent oscillators which would result in a complex and an expensive implementation. But these processes of modulation and demodulation are performed using the respective Inverse Fast Fourier Transform (IFFT) and Fast Fourier Transform (FFT). When sampling the complex envelope $x(t)$ of an OFDM symbol with rate $1/T_d$ the samples are given as

$$x_v = \frac{1}{N_c}\sum_{n=0}^{N_c-1} S_n e^{j2\pi nvt/N_c}, V = 0,\ldots,N_c - 1 \quad (2.5)$$

The sequence x_v ,$v = 0, \ldots, N_c - 1$ is the IDFT of the source symbol sequence. The block diagram in Fig. 2.2 depicts the modulator and the demodulator of OFDM[18].

2.1.1. Cyclic Prefix

One of the most important features of the OFDM technique is the way how OFDM deals with delays. As seen in (2.1) the duration of the OFDM symbol (T_{symbol}) increases by a factor of N_c and becomes larger than the duration of the impulse response τ_{max} of the channel and, thus the amount of Inter-Symbol Interference (ISI) decreases.

To completely avoid the effects of ISI and maintain the orthogonality between the sub-carriers, i.e., to avoid Inter-Carrier Interference (ICI), a guard interval also known as cyclic prefix must have at least the duration of τ_{max}

$$T_g \geq \tau_{\max} \quad (2.6)$$

This cyclic prefix must be inserted between adjacent OFDM symbols and each cyclic prefix is obtained by the extension of the OFDM symbol as seen in Fig. 2.3.

$$T_{symbol}' = T_g + T_b \quad (2.7)$$

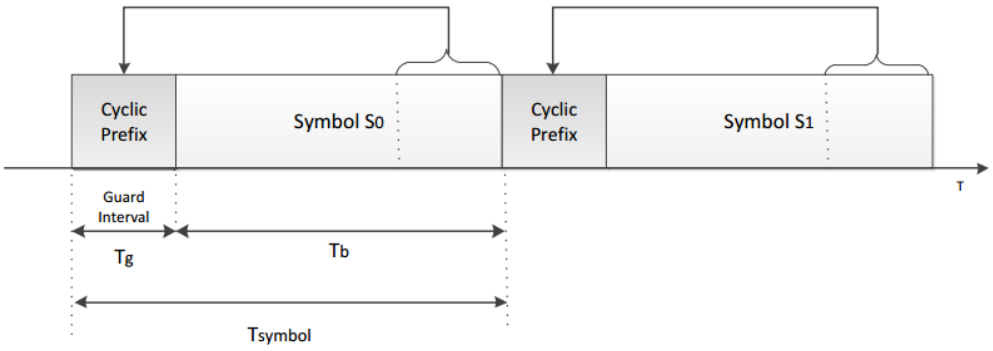

Fig. 2.3 Cyclic Prefix.

The discrete length of the guard interval has to be

$$L_g \geq \left\lceil \frac{\tau_{\max} N_c}{T_{symbol}} \right\rceil \tag{2.8}$$

And the sampled sequence with cyclic extended guard interval is

$$x_v = \frac{1}{N_c} \sum_{n=0}^{N_c-1} S_n e^{j2\pi nvt/N_c}, v = -L_g, ..., N_c - 1 \tag{2.9}$$

2.1.2. Advantages and Disadvantages of OFDM

This section summarizes the pros and cons of OFDM in the table 2.1.

Advantages: - High spectral efficiency for high numbers of sub-carriers. - Simple digital realization by using the FFT operation. - Low complex receivers due to avoidance of ISI and ICI with a long enough guard interval.
Disadvantages: - Multi-carrier signals with high PAPR. - Loss in spectral efficiency due to the guard interval. - More sensitive to Doppler spreads than single-carrier systems. - Needs accurate frequency and time synchronization.

Table 2.1 Advantages and Disadvantages of OFDM.

2.2. MC-CDMA

The combination of OFDM and CDMA has been subject to intensive research during the past years, and we already gave an overview in the introduction. Here, we describe with more detail both the transmitter and receiver of a MC-CDMA based system.

2.2.1. Signal Structure

The principle of MC-CDMA is to map the chips of a spread data symbols in frequency direction over several parallel sub-channels[18].

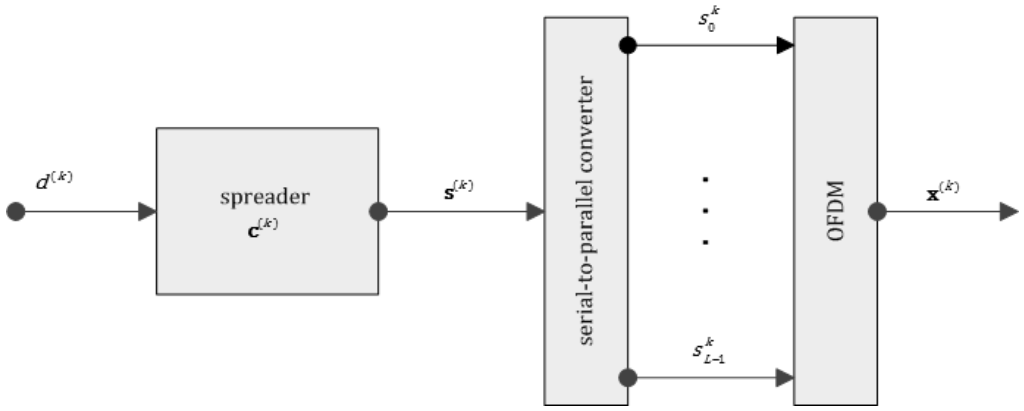

Fig. 2.4 Multi Carrier Spread Spectrum signal generation.

The Fig 2.4shows multi-carrier spectrum spreading of one complex-valued data symbol $d^{(k)}$ assigned to user k with a symbol rate of $1/T_d$.

In the transmitter, the complex data symbol $d^{(k)}$ is multiplied with the user specific spreading code

$$\mathbf{c}^{(k)} = (c_0^{(k)}, c_1^{(k)}, \ldots, c_{L-1}^{(k)})^T \tag{2.10}$$

The chip rate of the spreading code $c^{(k)}$ before serial-to-parallel conversion is

$$\frac{1}{T_c} = \frac{L}{T_d} \tag{2.11}$$

and it is$L$ times higher than the data symbol rate $1/T_d$. After the spreading is given by

$$\mathbf{s}^{(k)} = d^{(k)}\mathbf{c}^{(k)} = \left(s_0^k, s_1^k, ..., s_{L-1}^k\right) \tag{2.12}$$

a multi-carrier spread spectrum signal is obtained after modulating the components $s_l^k, l = 0,...,L-1$ in parallel sub-carriers.

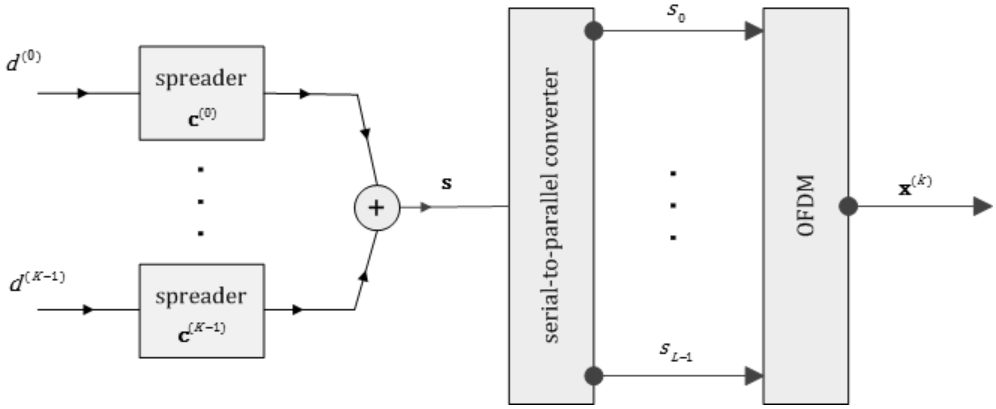

Fig. 2.5 MC-CDMA downlink transmitter.

In this thesis, it is used MC-CDMA to downlink operation. The Fig. 2.5 shows how it is performed the downlink where the spread signals of *K* users are added before the OFDM operation.

The sequence obtained is

$$\mathbf{s} = \sum_{k=0}^{K-1} \mathbf{s}^{(k)} = (s_0, s_1, ..., s_{L-1})^T \tag{2.13}$$

that can, also, be represented as

$$\mathbf{s} = \mathbf{C}\mathbf{d} \tag{2.14}$$

Where $\mathbf{d}$ is the vector with transmitted data symbols of the *K* active users and $\mathbf{C}$ is the spreading matrix. After processing the sequence through the OFDM block it is obtained the MC-CDMA downlink signal. Then, and as the OFDM system, a cyclic prefix or guard time is added as can be seen in Fig. 2.2 in OFDM block.

At the receiver depicted in Fig. 2.6, and assuming that the guard time is long enough to assure the signal is transmitted without ISI interference, the received vector after OFDM demodulation is given by

$$\mathbf{r} = \mathbf{H}\mathbf{s} + \mathbf{n} \tag{2.15}$$

Where $\mathbf{H}$ is the LxL channel matrix and $\mathbf{n}$ is the noise vector of length L with zero mean and variance σ^2.

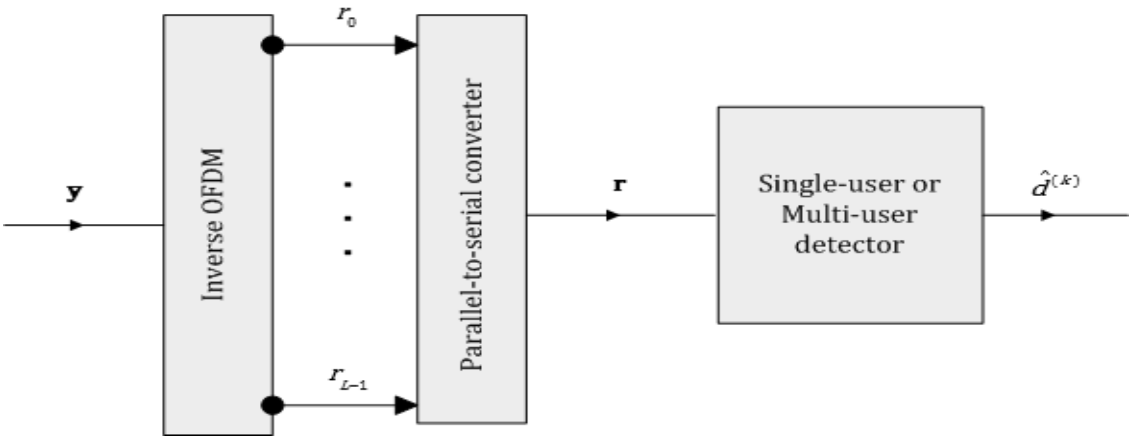

Fig. 2.6 MC-CDMA downlink receiver.

The estimates of the spreading signals are obtained after the equalization on the frequency domain. For that a standard linear zero forcing (ZF) or minimum mean square error (MMSE) can be employed. The equalization matrices can be given by

$$\mathbf{G}_{ZF} = \left[\mathbf{H}^{\mathrm{H}}\mathbf{H}\right]^{-1}\mathbf{H}^{\mathrm{H}} \tag{2.16}$$

$$\mathbf{G}_{MMSE} = \left[\mathbf{H}^{\mathrm{H}}\mathbf{H} + \sigma^2\mathbf{I}_L\right]^{-1}\mathbf{H}^{\mathrm{H}} \tag{2.17}$$

However, as briefly discussed in Chapter 1, this is not the best strategy since the residual interference levels might be too high, leading to performance that is still several dB from the matched filter bound.

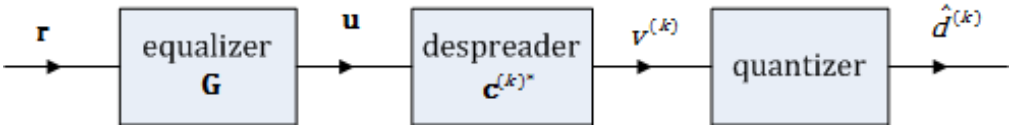

Fig. 2.7 MC-CDMA single user detection.

After equalization, the signals at each receiver are despreading by using the code employed at the transmitter. Finally, these signals are fed to the data detector in order to get hard estimate of the transmitted data.

The single user detection strategy presented in Fig. 2.7 is to detect the user signal of interest by not taking into account any information about the multiple access interference.
In the next Chapter will be discussed a more efficient equalization technique, based on the IB-DFE principle.

2.2.2. Advantages and Drawbacks of MC-CDMA

The main advantages and disadvantages of MC-CDMA are:

Advantages	Disadvantages
- Simple implementation with FFT - Low complex receivers - High spectral efficiency - High frequency diversity gain due to spreading in frequency direction	- High PAPR which is specially critic in the uplink - Synchronous transmission

Table 2.2 Advantages and Disadvantages of MC-CDMA.

3. Transmission and Detection Schemes

In this Chapter we start by giving an overview of MIMO bases systems, namely the diversity and multiplexing concepts. Then, we present the IB-DFE and IA concepts, techniques used to derive the proposed schemes.

3.1. Multi Input Multi Output

MIMO systems have advantage over the SISO systems in a way that MIMO systems improve the throughput and the capacity of the wireless link by transmitting multiple streams of data in parallel and using diversity techniques. Another advantage is the reduced interference between network users by using smart antennas.

There are other arrangements capable of implementing LTE without the use of multiple antennas in the transmission and reception. As the name suggests, SISO only uses two antennas, one for transmission and another for reception. The MISO system provides multiple antennas for transmission and one for reception. The other possible combination is the SIMO system which uses one antenna in the transmitter and multiple antennas in the receiver.

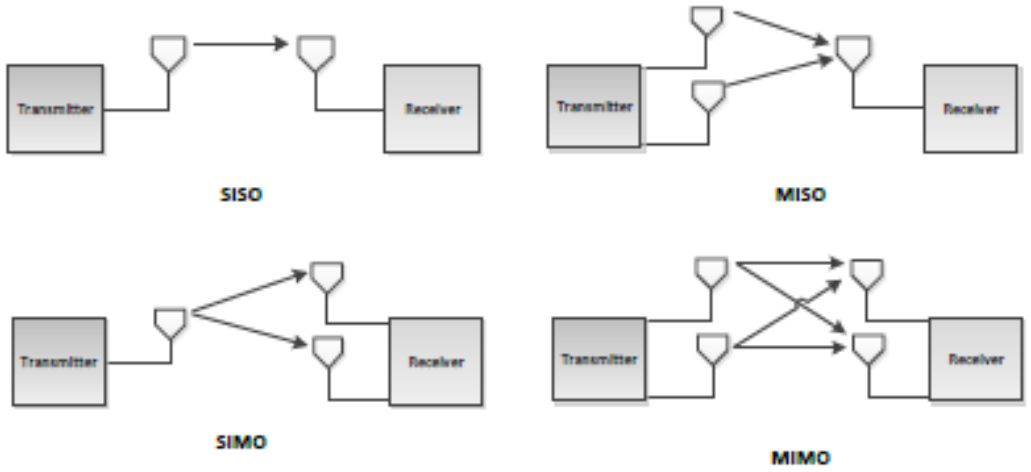

Fig. 3.1 MIMO scenarios.

Although all of these schemes provide good communication systems, in practice, the transmission channel is affected by reflection, diffusion and refraction effects. Those effects generate different paths for the transmitted data which are received with temporal variation of amplitude and phase. The effectiveness of diversity schemes lies in the fact that at the receiver we must provide independent samples of the basic signal that was transmitted. Since the probability of two or more relevant parts of the signal undergoing deep fades will be very small we will get a diversity gain. The receiver must combine the received diversified waveforms to maximize the resulting signal quality. Transmit diversity is easier to implement at the BS and consists in introducing controlled redundancies at the transmitter, which can be then exploited by appropriate signal processing techniques at the receiver .

Considering all previous systems, the MIMO configuration is the only with the ability to perform spatial multiplexing using multiple antennas. In this way, the transmission rate increases with the antenna pairs.

The Signal to Interference-plus-Noise Ratio (SINR) variation is a common scenario in the MIMO systems which have different objectives in case the SINR is high, in which the main objective is to share de SINR and when it is low, the objective is to improve it.

When low SINR occurs, the generation of a narrow beam in the direction of the receiver and the transmission use diversity techniques. Although transmission diversity does not

improve the average SINR, it reduces the variations in the SINR experienced by the receiver, enabling the use of high order modulations and increase the coding rate, obtaining a higher link throughput[21].

For the case when the SINR is high it is not worth of increasing it further because the throughput curve saturates. To prevent such effect, multiple antennas are used at the transmitter and receiver of the radio link. This allows spatial multiplexing where different information bits are sent from each antenna, sharing overall SINR.

3.2. Iterative Block Decision Feedback Equalizer

Despite the reasonable complexity/performance commitment obtained with linear equalizers schemes, they still have to deal with several problems inherent to its own nature, namely noise enhancement and residual ISI. It is well-known that nonlinear equalization outperforms the linear approach. Among nonlinear equalizers the DFE is a popular choice since it provides a good trade-off between complexity and performance. A basic structure is depicted in Fig. 3.2. The nonlinear equalizer DFE is implemented through a feedback filter to the output of the feedforward block samples, and associating this process to an iterative scheme, makes the DFE an efficient way of equalizing the received signals. Thus, an iterative-Block Decision Feedback Equalizer is obtained, which corresponds to an iterative DFE where the feedforward and feedback operations are implemented in the frequency domain, as depicted in Fig. 3.2[22].

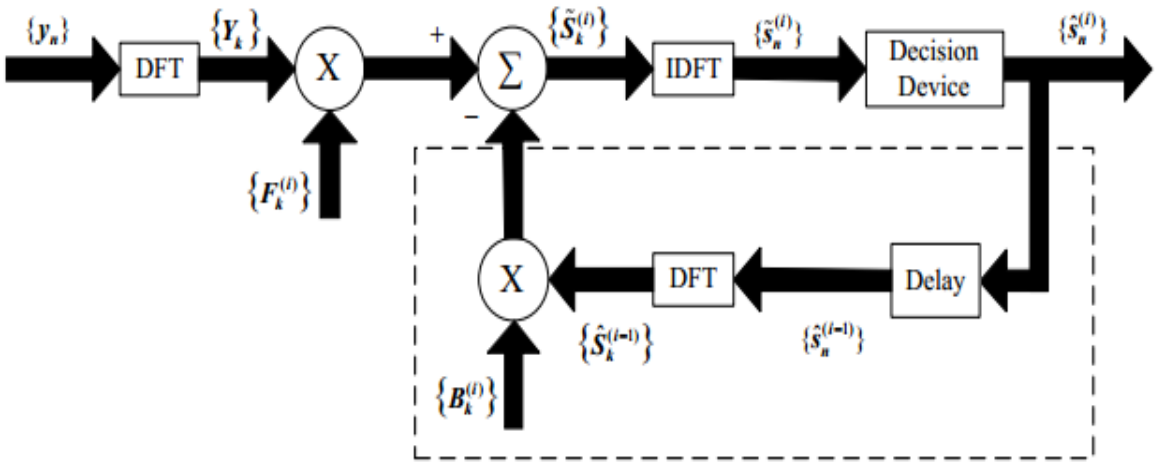

Fig. 3.2 Basic IB-DFE block diagram for single carrier system in frequency domain and assuming single user.

From the Fig. 3.2 we can see that at the i^{th} iteration, the frequency-domain block at the output of the equalizer is

$$\tilde{\mathbf{S}}_k^{(i)} = \mathbf{F}_k^{(i)}\mathbf{Y}_k - \mathbf{B}_k^{(i)}\hat{\mathbf{S}}_k^{(i-1)} \tag{3.1}$$

Where $\mathbf{F}_{\mathrm{k}}^{(\mathrm{i})}$ is the feedforward coefficient and $\mathbf{B}_{\mathrm{k}}^{(\mathrm{i})}$ the feedback coefficient from the DFE block.

The feedforward and feedback coefficients are chosen in order to maximize the SINR is given by

$$\mathbf{F}_k^{(i)} = \frac{\mathbf{H}_k^*}{\sigma^2 + (1 - \left(\rho^{(i-1)}\right)^2)\left|\mathbf{H}_k\right|^2} \tag{3.2}$$

and

$$\mathbf{B}_k^{(i)} = \rho^{(i-1)}(\mathbf{F}_k^{(i)}\mathbf{H}_k - 1), \tag{3.3}$$

respectively. The ρ factor corresponds to the correlation coefficient and represents a crucial parameter to ensure a good performance at the receiver, since it supplies a reliability measure of the estimates employed at the feedback loop.

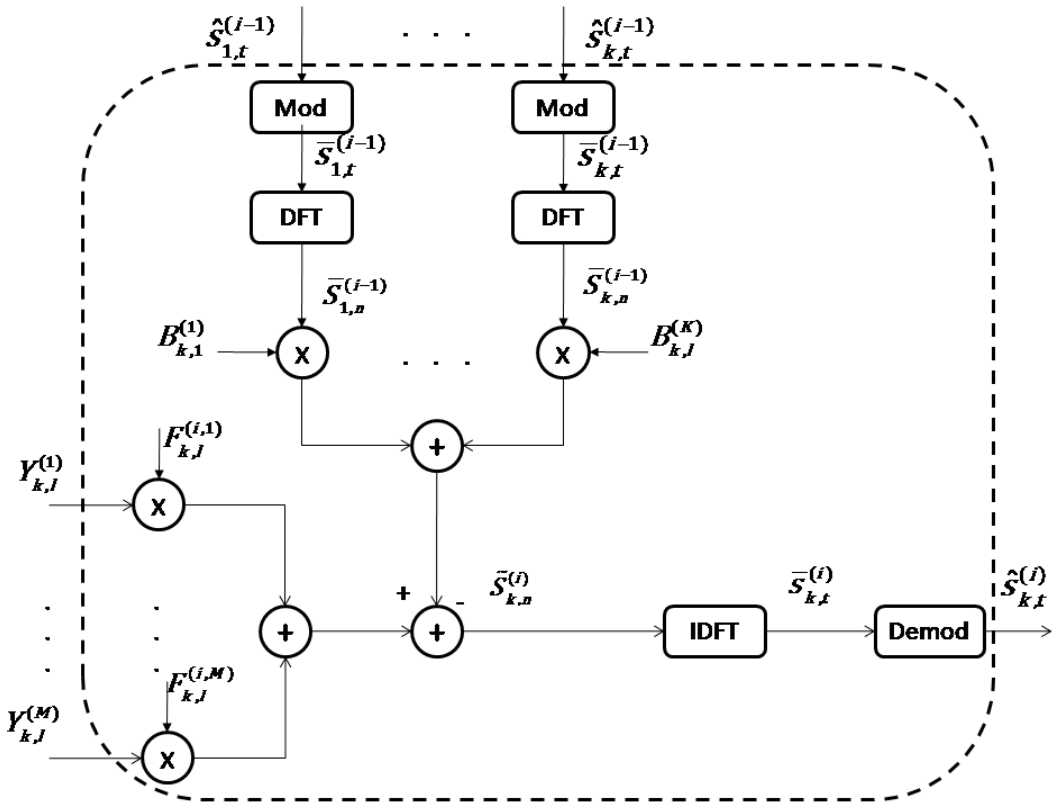

Fig. 3.3 IB-DFE for the k^{th} user assuming *M* received antennas.

The system depicted in Fig. 3.3 with multiple users and multiple antennas was studied in [15]. Considering a matrix notation we have

$$\mathbf{Y}_{k,l} = \mathbf{H}_{k,l}^{(i)\mathrm{T}} \mathbf{S}_{k,l} - \mathbf{N}_{k,l} \tag{3.4}$$

Where $\mathbf{Y}_{k,l}$ is a column vector where each line corresponds to the received signal,

$$\mathbf{Y}_{k,l} = \begin{bmatrix} Y_{1,l}^{(1)} \\ Y_{2,l}^{(2)} \\ \vdots \\ Y_{k,l}^{(\mathrm{M})} \end{bmatrix}, \tag{3.5}$$

$\mathbf{S}_{k,l}$ is a *K* column vector where each element represents the transmitted data in the frequency for each user at the subcarrier *l*,

$$\mathbf{S}_{k,l} = \begin{bmatrix} S_{1,l} \\ S_{2,l} \\ \vdots \\ S_{k,l} \end{bmatrix}, \tag{3.6}$$

$\mathbf{N}_{k,l}$ is a *M* column vector containing the noise samples received at each antenna,

$$\mathbf{N}_{k,l} = \begin{bmatrix} N_{1,l}^{(1)} \\ N_{2,l}^{(2)} \\ \vdots \\ N_{k,l}^{(\mathrm{M})} \end{bmatrix}, \tag{3.7}$$

And$\mathbf{H}_{k,l}$ is a *KxM* matrix containing the channel frequency response, defined by

$$\mathbf{H}_{k,l} = \begin{bmatrix} H_{1,l}^{(1)} & H_{1,l}^{(2)} & \dots & H_{1,l}^{(M)} \\ H_{2,l}^{(1)} & H_{2,l}^{(2)} & \dots & H_{2,l}^{(M)} \\ \vdots & \vdots & \ddots & \vdots \\ H_{k,1}^{(1)} & H_{k,l}^{(2)} & \dots & H_{k,l}^{(M)} \end{bmatrix}. \tag{3.8}$$

Considering an IB-DFE receiver where each iteration consists of *K* detection stages, one for each user. To detect thek^{th} user at the i^{th} iteration, the following method is applied.

The result samples $\tilde{\mathbf{S}}_{k,l}$ for each iteration, in matrix format, is given by,

$$\tilde{\mathbf{S}}_{k,l}^{(i)} = \mathbf{F}_{k,l}^{(i)\mathrm{T}} \mathbf{Y}_{k,l} - \mathbf{B}_{k,l}^{(i)\mathrm{T}} \bar{\mathbf{S}}_{k,l}^{(i-1)}, \tag{3.9}$$

Where $\bar{\mathbf{S}}_{k,l}$ is the vector with the soft decisions of $\mathbf{S}_{k,l}$ from the previous iteration, $\mathbf{F}_{k,l}^{(i)}$ is a *MxK* matrix containing the forward coefficients and $\mathbf{B}_{k,l}^{(i)}$ the *KxK* feedback coefficients. The feedforward and the feedback matrices, $\mathbf{F}_{k,l}^{(i)}$ and $\mathbf{B}_{k,l}^{(i)}$ in matrice notation, are chosen to maximize the SINR for each user is given by

$$\mathbf{F}_{k,l}^{(i)} = \left[\mathbf{H}_{k,l}^{\mathrm{H}} \left(\mathbf{I}_{\mathrm{p}} - \mathbf{R}^{(i-1)^2}\right) \mathbf{H}_{k,l} + \sigma^2 \mathbf{I}_M\right]^{-1} \mathbf{H}_{k,l}^{\mathrm{H}} \mathbf{Q} \tag{3.10}$$

Where $\mathbf{R}_k^{(i)} = diag\left[\rho_{k,1}^{(i)} \quad \dots \quad \rho_{k,P}^{(i)}\right]$ is a diagonal correlation matrix computed at *i*th iteration, where the correlation coefficient computed for the *p*th *L*-length data block is

$$\rho_k = \frac{\mathbb{E}\left[\bar{s}_{k,l} s_{k,l}^*\right]}{\mathbb{E}\left[\left|s_{k,l}\right|^2\right]} \quad , l = 1,\dots,L, \tag{3.11}$$

$\sigma^2$is the noise variance and $\mathbf{Q} = diag\left[Q_1 \quad \dots \quad Q_k\right]$ represents the normalization diagonal matrix to ensure that

$$\frac{Q_p}{L} \sum_{l=0}^{L-1} \sum_{m=1}^{M} F_{k,l}^{(m,i)} H_{k,l}^{(m)} = 1 \tag{3.12}$$

and

$$\mathbf{B}_{k,l}^{(i)} = (\mathbf{H}_{k,l}\mathbf{F}_{k,l}^{(i)} - \mathbf{I}_{\mathrm{p}}) \tag{3.13}$$

3.3. Interference Alignment

As briefly discussed in Chapter 1, analysis of interference channels has shown that capacity of an interference channel for a given user is half the rate of its interference-free capacity in the high transmit power regime, for any number of users. One recent scheme to efficiently eliminate the multiuser interference and achieve a linear capacity scaling is interference alignment.

Considering a system of linear equation

$$\begin{aligned}
\mathbf{y}_1 &= \mathbf{H}_{11}\mathbf{x}_1 + \mathbf{H}_{12}\mathbf{x}_2 + \ldots + \mathbf{H}_{1K}\mathbf{x}_K \\
\mathbf{y}_2 &= \mathbf{H}_{21}\mathbf{x}_1 + \mathbf{H}_{22}\mathbf{x}_2 + \ldots + \mathbf{H}_{2K}\mathbf{x}_K \\
&\vdots \quad \vdots \quad \vdots \\
\mathbf{y}_B &= \mathbf{H}_{B1}\mathbf{x}_1 + \mathbf{H}_{B2}\mathbf{X}_2 + \ldots + \mathbf{H}_{BK}\mathbf{x}_K \ ,
\end{aligned} \tag{3.14}$$

Where we have *B* observations $\mathbf{y}_1, \mathbf{y}_2, \ldots, \mathbf{y}_{\mathrm{B}}$, each in the form of a linear combination of *K* information symbols $\mathbf{x}_1, \mathbf{x}_2, \ldots, \mathbf{x}_{\mathrm{B}}$ with coefficients $\mathbf{H}_{ij}$. Thus, we can interpret *K* as the number of transmitters, each one trying to send an information symbol and the coefficients $\mathbf{H}_{ij}$ as the effective channel coefficients. *B* is the bandwidth or the number of signaling dimensions accessible at a receiver through a linear channel. Since the channel is linear, each signaling dimension produces a linear combination of the transmitted information symbols. This means that a receiver has access to *B* signaling dimensions. In this case, we are interested in interference networks where only a subset of symbols are desired by the receiver and the remaining symbols are the undesired symbols at the correspondent receiver.

If we consider the following linear equation:

$$\mathbf{y} = \mathbf{H}_{*1}\mathbf{x}_1 + \mathbf{H}_{*2}\mathbf{x}_2 + \ldots + \mathbf{H}_{*k}\mathbf{x}_k \tag{3.15}$$

Where $\mathbf{y}$ and $\mathbf{H}_{*k}$ are the observation vector and $\mathbf{H}_{*k}$ the signaling dimension of the symbol $\mathbf{x}_k$, respectively. In MIMO systems, we call the vector $\mathbf{H}_{*k}$ the received beam direction for symbol $\mathbf{x}_k$.

Thus, the condition for recover the desired symbol $\mathbf{x}_1$ from the observation vector Y is the received beam for $\mathbf{x}_1$,i.e., $\mathbf{H}_{*1}$ should not be contained in the vector spanned by the undesired beams $\mathbf{H}_{*2}\mathbf{x}_2, \ldots, \mathbf{H}_{*k}\mathbf{x}_k$, the receiver can recover $\mathbf{x}_1$ if and only if

$$\mathbf{H}_{*1}\text{span} \notin (\mathbf{H}_{*2}\mathbf{x}_2, \ldots, \mathbf{H}_{*k}\mathbf{x}_k). \tag{3.16}$$

So, if the interference beams could be constrained into a smaller subspace, then they do not span the entire available signal space at the receiver and the desired signal beam could avoid the interference space and the receiver could recover its desired symbol.

In Fig. 3.4 we present the IA system for 3 users. It comprises 3 transmitter-receiver pairs sharing the same physical channel, where a given transmitter only intends to have its signal decoded by a single receiver. An IA closed form solution was studied and presented for 3 users in [17].

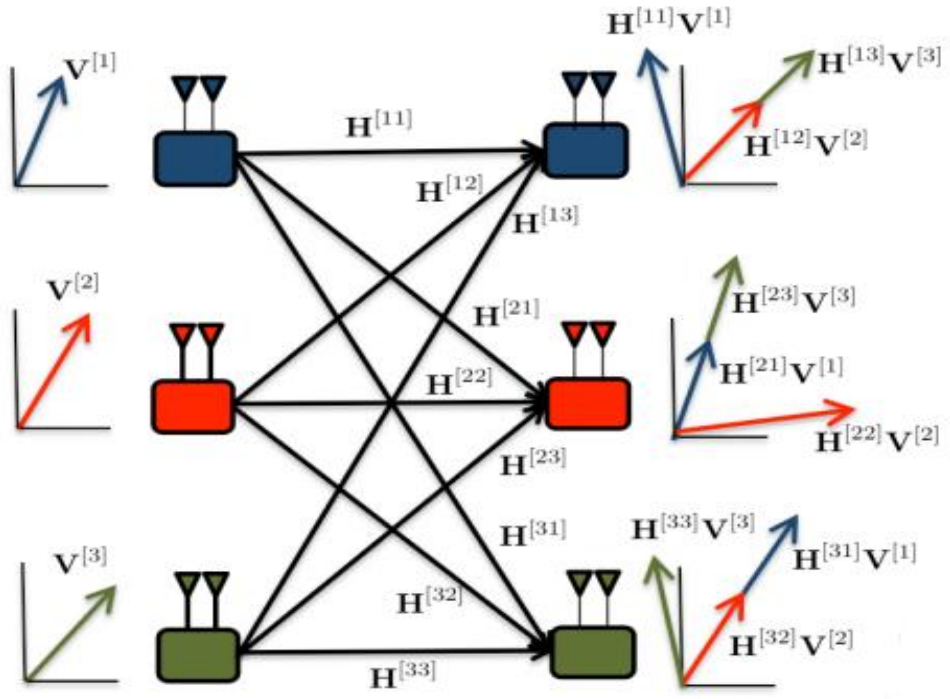

Fig. 3.4 Interference Alignment on the user 3 User MIMO Interference Channel with 2 antennas.

For this particular 3-user system the alignment condition for each emitter-receiver pair are:

Interference alignment at receiver 1

$\mathbf{H}^{[12]}\mathbf{V}^{[2]} \equiv \mathbf{H}^{[12]}\mathbf{V}^{[3]}$

$$\Rightarrow \mathbf{V}^{[2]} \equiv (\mathbf{H}^{[12]})^{-1}\mathbf{H}^{[13]}\mathbf{V}^{[3]} \tag{3.17}$$

Interference alignment at receiver 2

$\mathbf{H}^{[21]}\mathbf{V}^{[1]} \equiv \mathbf{H}^{[23]}\mathbf{V}^{[3]}$

$$\Rightarrow \mathbf{V}^{[1]} \equiv (\mathbf{H}^{[21]})^{-1}\mathbf{H}^{[23]}\mathbf{V}^{[3]} \tag{3.18}$$

Interference alignment at receiver 3

$\mathbf{H}^{[31]}\mathbf{V}^{[1]} \equiv \mathbf{H}^{[32]}\mathbf{V}^{[2]}$

$$\mathbf{H}^{[31]}(\mathbf{H}^{[21]})^{-1}\mathbf{H}^{[23]}\mathbf{V}^{[3]} \equiv \mathbf{H}^{[32]}(\mathbf{H}^{[12]})^{-1}\mathbf{H}^{[13]}\mathbf{V}^{[3]} \tag{3.19}$$

$$\mathbf{V}^{[3]} = \mathrm{eigvec}\left(\left(\mathbf{H}^{[23]}\right)^{-1}\mathbf{H}^{[21]}\left(\mathbf{H}^{[31]}\right)^{-1}\mathbf{H}^{[32]}\left(\mathbf{H}^{[12]}\right)^{-1}\mathbf{H}^{[13]}\mathbf{V}^{[3]}\right) \tag{3.20}$$

In a three user interference channel, transmitter 1's signal needs to align with transmitter 2's signal at receiver 3, and with transmitter 3's signal at receiver 2. This creates a chain of alignment conditions that in the end folds upon itself, as shown in Fig. 3.4.

In this thesis, it will be used the closed solution of three user MIMO Channel with 2 or 4 antenna. Note that closed form solution for more than 3 users has not derived yet. Solutions for more than 3 users only exist considering iterative alignment techniques [23].

4. IB-DFE with IA for MC-CDMA systems

As discussed, IA is a promising technique that allows high capacity gains in interfering channels. On the other hand, iterative frequency-domain detection receivers based on the IB-DFE concept can efficiently exploit the inherent space-frequency diversity of the MIMO MC-CDMA systems. Therefore, in this thesis we consider IA precoding at the transmitter with IB-DFE at the receiver for MIMO MC-CDMA systems. To the best of our knowledge joint IA-precoding and IB-DFE for MC-CDMA systems has not been addressed in the literature. In the proposed scheme the chips are IA-precoded instead of the data symbols as in the narrowband or OFDM systems. The receiver is designed in two steps: first standard ZF and MMSE equalizers are used to mitigate the aligned users´ interference, then and after a whitening noise process, an IB-DFE based equalizer is designed to mitigate both the residual inter-user and inter-carrier interferences. The proposed scheme achieves the maximum degrees of freedom, while allowing a close-to-optimum diversity gain, with only a few iterations at the receiver side.

The remainder of the Chapter is organized as follows: section 4.1 presents the MIMO IA-precoded MC-CDMA system model. Section 4.2 starts by briefly presenting the iterative IA-precoding considered in this paper. Then, the proposed receiver structure is presented in detail. Section 4.3 presents the main performance results.

4.1. System Characterization

Let's consider a *K*-user MIMO interference channels where a *K* transmitter-receiver pair share the same physical channel, where a given transmitter only intends to have its signal decoded by a single receiver.

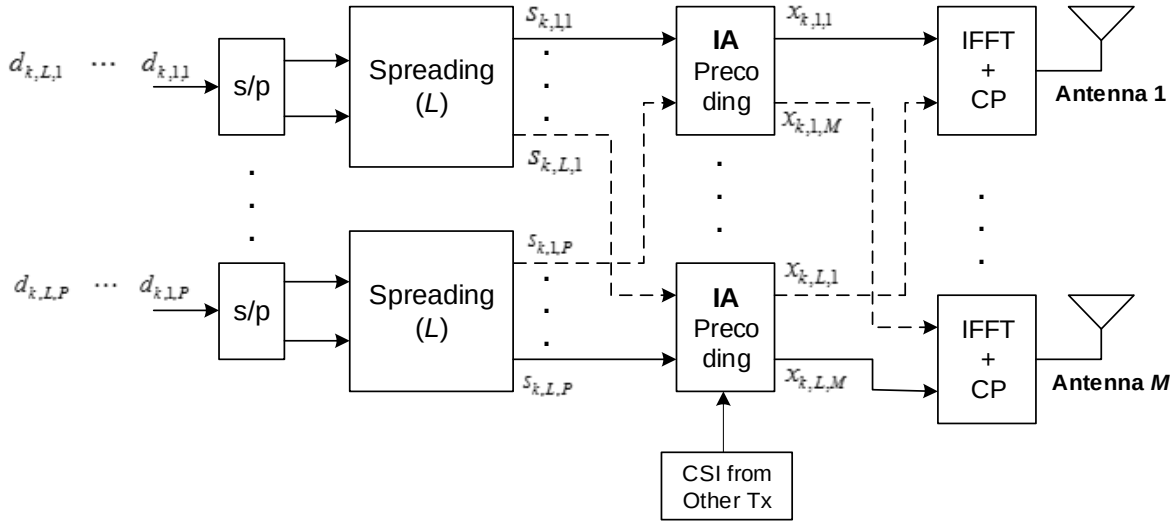

Fig. 4.1 MC-CDMA transmitter with interference alignment.

It is considered a symmetric case where all transmitters and receivers have *M* antennas. Since each transmitter is allowed to transmit *P=M/2* data symbols on each sub-carrier, this system has *KM/2*. Fig. 1 shows the proposed system k^{th} MC-CDMA based transmitter. As can be seen in Fig. 4.1, each one of the *P* blocks of *L* data symbols are spread into *L* chips using orthogonal Walsh-Hadamard codes. The transmit signal of the p^{th} data block, after the spreading operation is

$$\mathbf{s}_k^p = \mathbf{C}\mathbf{d}_k^p = \begin{bmatrix} s_{k,1,p} & \cdots & s_{k,L,p} \end{bmatrix}^T \quad ,l = 1,...,L,\ p = 1,...,P, \tag{4.1}$$

Where **C** is a square spreading code matrix of size *L x L* and $\mathbf{d}_k^p$ is a data vector of the p^{th} block of size *L* with $\mathbb{E}\left[\mathbf{d}_k^p \mathbf{d}_k^{pH}\right] = \mathbf{I}_L$. Then, a set of P chips (one of each block) is weighted by an IA-precoding matrix. IA-precoding is applied on a chip level instead of data level. The signal after the IA precoding on sub-carriers l can be written as,

$$\mathbf{x}_{k,l} = \mathbf{W}_{k,l}\mathbf{s}_{k,l} \tag{4.2}$$

Where $\mathbf{W}_{k,l} \in \mathbb{C}^{MxP}$ is the linear precoding matrix computed at the transmitter *k* on subcarrier *l*, constrained to $\|\mathbf{W}_{k,l}\|_F^2 \leq T_p$ and T_p is the transmit power with $\mathbf{s}_{k,l} = \begin{bmatrix} s_{k,l,1} & \cdots & s_{k,l,P} \end{bmatrix}^T$. Then, the precoding signals are mapped into the OFDM frame and the cyclic prefix is inserted.

The received signal, in the frequency domain, at the user k^{th} on the subcarrier *l* can be written as

$$\mathbf{y}_{k,l} = \mathbf{H}_{k,k,l}\mathbf{W}_{k,l}\mathbf{s}_{k,l} + \sum_{\substack{j=1 \\ j \neq k}}^{K} \mathbf{H}_{k,j,l}\mathbf{W}_{j,l}\mathbf{s}_{j,l} + \mathbf{n}_{k,l} \tag{4.3}$$

considering that the cyclic prefix is long enough to take into account the overall channel impulse responses such as the transmit and receive filters, multipath propagation effects and variance in the time-of-arrival for different transmitter-to-receiver links.

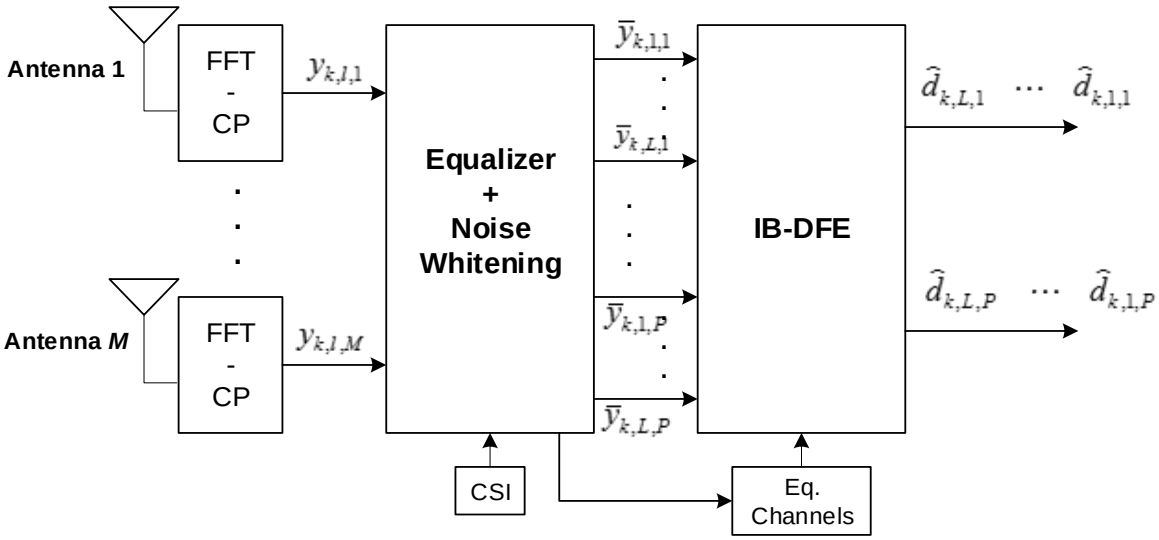

Fig. 4.2 MC-CDMA receiver with IB-DFE.

As can be seen from Fig. 4.2, the detection procedure is performed in two steps: firstly, it is done the equalizer process where it is used zero forcing (ZF) or minimum mean square error (MMSE) to remove the aligned user's interference. After this equalization, the signal is given by

$$\tilde{\mathbf{y}}_{k,l} = \mathbf{G}_{k,l}\mathbf{H}_{k,k,l}\mathbf{W}_{k,l}\mathbf{s}_{k,l} + \mathbf{G}_{k,l}\sum_{\substack{j=1 \\ j\neq k}}^{K}\mathbf{H}_{k,j,l}\mathbf{W}_{j,l}\mathbf{s}_{j,l} + \mathbf{G}_{k,l}\mathbf{n}_{k,l} \quad (4.4)$$

Where $\mathbf{G}_{k,l} \in \mathbb{C}^{PxM}$ is the linear receiving filter with dimension *P x M*. Then, it is performed a noise whitening process over (4.4) to obtain the signal $\bar{\mathbf{y}}_{k,l}$. Secondly, an IB-DFE is designed, based on the equivalent channels provided by the first block and applied to $\bar{\mathbf{y}}_{k,l}$ to mitigate the inter-carrier interference.

4.2. Precoder and Equalizers Design

In this section, it is presented the closed-form IA precoding algorithm for $K \leq 3$ discussed in previous chapter. Then, the equalizers ZF and MMSE are used in order to remove the aligned user's interference and, finally, an IB-DFE is performed to remove the inter-carrier interference through parallel interference cancelation (PIC) approach.

4.2.1 IA Precoder for $K \leq 3$

A closed-form solution is possible for a three user interference channel, $\mathbf{W}_{k,l}, k = 1,2,3$. As shown in (4.5), the solution for subcarrier *l* is given by,

$$\begin{aligned} \mathbf{W}_{1,l} &= \begin{bmatrix} \omega_1 & \omega_2 & \dots & \omega_{M/2} \end{bmatrix} \\ \mathbf{W}_{2,l} &= \mathbf{H}_{3,2,l}^{-1}\mathbf{H}_{3,1,l}\mathbf{W}_{1,l} \\ \mathbf{W}_{3,l} &= \mathbf{H}_{2,3,l}^{-1}\mathbf{H}_{2,1,l}\mathbf{W}_{1,l} \end{aligned} \quad (4.5)$$

Where $\omega_1, \omega_2, \dots, \omega_{M/2}$ are the eigenvectors of matrix $\boldsymbol{\omega}_l = \mathbf{H}_{3,1,l}^{-1}\mathbf{H}_{3,2,l}\mathbf{H}_{1,2,l}^{-1}\mathbf{H}_{1,3,l}\mathbf{H}_{2,3,l}^{-1}\mathbf{H}_{2,1,l}$.

4.2.2 Equalizers Design

The first step of the detector procedure consists in the removal of the aligned user's interference. In this thesis, it is performed through both ZF and MMSE based equalizers.

a) ZF based equalizer

The ZF equalizer is given by,

$$\bar{\mathbf{G}}_{k,l} = \left(\mathbf{H}_{t,k,l}^{H}\mathbf{H}_{t,k,l}\right)^{-1}\mathbf{H}_{t,k,l}^{H} \tag{4.6}$$

where $\mathbf{H}_{t,k,l} = \left[\mathbf{H}_{k,1,l}\mathbf{W}_{1,l} \;\; \mathbf{H}_{k,2,l}\mathbf{W}_{2,l} \;\; \mathbf{H}_{k,3,l}\mathbf{W}_{3,l}\right]$ is of size $(M \times 3P)$. The left pseudo-inverse exists since $\mathbf{H}_{t,k,l}$ has *M* column rank due to the IA processing. From (4.6), the linear filter used at the k^{th} receiver on p^{th} sub-carrier is given by,

$$\mathbf{G}_{k,l} = \left[\mathbf{g}^{T}_{k,\frac{(k-1)M}{2}+1,l} \quad \mathbf{g}^{T}_{k,\frac{(k-1)M}{2}+2,l} \quad \cdots \quad \mathbf{g}^{T}_{k,\frac{(k-1)M}{2}+\frac{M}{2},l}\right]^{T} \tag{4.7}$$

where $\mathbf{g}_{k,j,l}$ is the j^{th} row vector of $\bar{\mathbf{G}}_{k,l}$. Replacing (4.7) in (4.4) the received signal is reduced to,

$$\tilde{\mathbf{y}}_{k,l} = \mathbf{s}_{k,l} + \mathbf{G}_{k,l}\mathbf{n}_{k,l} \tag{4.8}$$

Now, it is necessary to apply a noise whitening process. The noise covariance is given by,

$$\mathbb{E}\left[\mathbf{G}_{k,l}\mathbf{n}_{k,l}\mathbf{n}_{k,l}^{H}\mathbf{G}_{k,l}^{H}\right] = \sigma^{2}\mathbf{G}_{k,l}\mathbf{G}_{k,l}^{H} \tag{4.9}$$

to make the noise white, a Cholesky factorization is applied,

$$\mathbf{G}_{k,l}\mathbf{G}_{k,l}^{H} = \mathbf{U}_{k,l}\mathbf{U}_{k,l}^{H} \tag{4.10}$$

where $\mathbf{U}_{k,l}$ is an upper triangular matrix.

Filtering (4.8) by $\left(\mathbf{U}_{k,l}\right)^{-1}$, the signal obtained at the input of the IB-DFE block is,

$$\bar{\mathbf{y}}_{k,l} = \left(\mathbf{U}_{k,l}\right)^{-1}\mathbf{s}_{k,l} + \left(\mathbf{U}_{k,l}\right)^{-1}\mathbf{G}_{k,l}\mathbf{n}_{k,l} \tag{4.11}$$

b) MMSE based equalizer

The MMSE equalizer is given by,

$$\bar{\mathbf{G}}_{k,l} = \left(\mathbf{H}_{t,k,l}^{H}\mathbf{H}_{t,k,l} + \mathbf{I}_{\frac{3M}{2}}\sigma^{2}\right)^{-1}\mathbf{H}_{t,k,l}^{H} \tag{4.12}$$

Where $\mathbf{H}_{t,k,l} = \left[\mathbf{H}_{k,1,l}\mathbf{W}_{1,l} \;\; \mathbf{H}_{k,2,l}\mathbf{W}_{2,l} \;\; \mathbf{H}_{k,3,l}\mathbf{W}_{3,l}\right]$ is of size $(M \times 3P)$.

Applying $\left(\mathbf{U}_{k,l}\right)^{-1}$ to (4.4) and after the same process in (4.10), the signal obtained at the input of the IB-DFE block is

$$\bar{\mathbf{y}}_{k,l} = \left(\mathbf{U}_{k,l}\right)^{-1}\mathbf{G}_{k,l}\mathbf{H}_{kk,l}\mathbf{W}_{k,l}\mathbf{s}_{k,l} + \sum_{j=1,\, j\neq k}^{K}\left(\mathbf{U}_{k,l}\right)^{-1}\mathbf{G}_{k,l}\mathbf{H}_{kj,l}\mathbf{W}_{j,l}\mathbf{s}_{j,l} + \left(\mathbf{U}_{k,l}\right)^{-1}\mathbf{G}_{k,l}\mathbf{n}_{k,l} \quad (4.13)$$

That can be written as,

$$\bar{\mathbf{y}}_{k,l} = \mathbf{H}^{T}_{eq,kk,l}\mathbf{s}_{k,l} + \sum_{j=1,\, j\neq k}^{K}\mathbf{H}^{T}_{eq,kj,l}\mathbf{s}_{j,l} + \left(\mathbf{U}_{k,l}\right)^{-1}\mathbf{G}_{k,l}\mathbf{n}_{k,l} \quad (4.14)$$

with

$$\mathbf{H}_{eq,kk,l} = \left[\left(\mathbf{U}_{k,l}\right)^{-1}\mathbf{G}_{k,l}\mathbf{H}_{kk,l}\mathbf{W}_{k,l}\right]^{T} \quad (4.15)$$

and

$$\mathbf{H}_{eq,kj,l} = \left[\left(\mathbf{U}_{k,l}\right)^{-1}\mathbf{G}_{k,l}\mathbf{H}_{kj,l}\mathbf{W}_{j,l}\right]^{T} \quad (4.16)$$

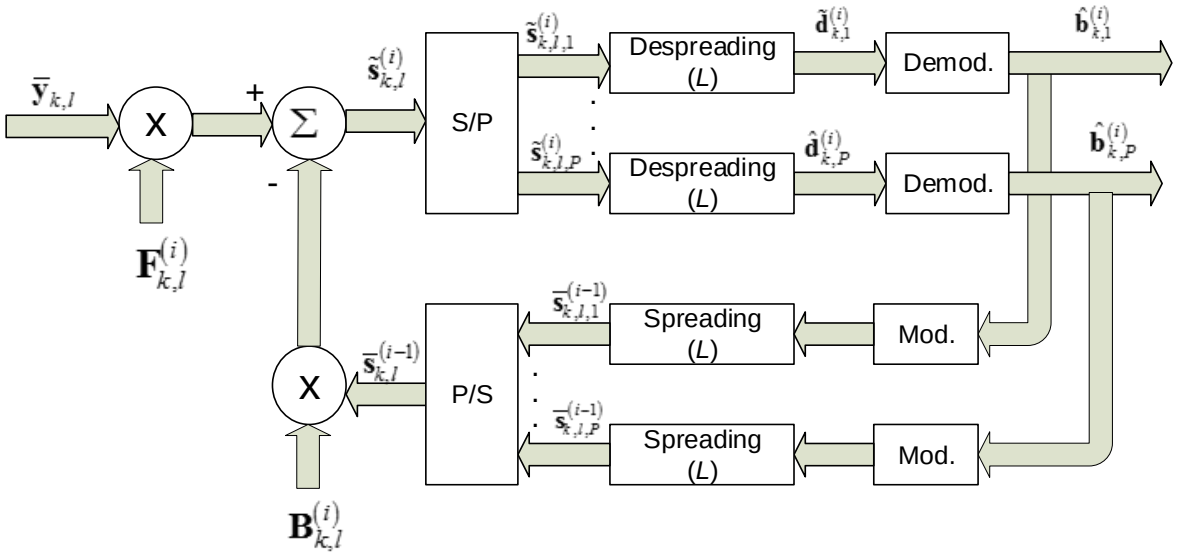

Fig. 4.3 IB-DFE block.

The second step consists in an iterative frequency domain equalizer based on IB-DFE processing. Fig. 4.3 shows the main blocks of the IB-DFE process. For each iteration we detect all *P* signals of the k^{th} user on l^{th} sub-carrier, in a parallel way, using the most updated estimate of the transmitted data symbols to cancel the residual interference, which could not be cancelled in the first equalizer block. Thus, our receiver can be

regarded as an iterative parallel interference cancellation (PIC). At the i^{th} iteration, the signal at k^{th} receiver on l^{th} subcarrier, before the despreading operation is given by,

$$\tilde{\mathbf{s}}_{k,l}^{(i)} = \mathbf{F}_{k,l}^{(i)T}\mathbf{y}_{k,l} - \mathbf{B}_{k,l}^{(i)T}\bar{\mathbf{s}}_{k,l}^{(i-1)} \tag{4.17}$$

With $\mathbf{F}_{k,l}^{(i)} \in \mathbb{C}^{PxP}$ denoting the feedforward matrix and $\mathbf{B}_{k,l}^{(i)T} \in \mathbb{C}^{PxP}$ is the feedback matrix. It can be shown that $\bar{\mathbf{s}}_{k,l}^{(i-1)} \approx \mathbf{R}_k^{(i)2}\mathbf{s}_{k,l} + \mathbf{R}_k^{(i)}\mathbf{e}_{k,l}$, where $\mathbf{e}_{k,l}$ is a zero mean error vector. For the first iteration, i.e., $i=1$, $\bar{\mathbf{s}}_{k,l}^{(0)}$ is a null vector and $\mathbf{R}_k^0$ is a null matrix. $\mathbf{R}_k^{(i)} = diag\left[\rho_{k,1}^{(i)} \quad \dots \quad \rho_{k,P}^{(i)}\right]$ is a diagonal correlation matrix computed at i^{th} iteration, where the correlation coefficient computed for the p^{th} data block is

$$\rho_{k,p}^{(i)} = \frac{\mathbb{E}\left[\hat{d}_{k,l,p}d_{k,l,p}^{*}\right]}{\mathbb{E}\left[\left|d_{k,l,p}\right|^2\right]} \quad ,l=1,\dots,L \tag{4.18}$$

a measure of the reliability of the estimates of the p^{th} data block associated to the i^{th} iteration.

The feedforward and feedback matrices are computed by minimizing the mean square error (MSE) between $\mathbf{s}_{k,l}$ and $\tilde{\mathbf{s}}_{k,l}^{(i)}$. Different solutions for the feedforward matrix are obtained depending of the equalizer technique used at the first receiver step:

c) ZF equalizer

Considering ZF at the first detection block we have the following feedforward and feedback matrices

$$\mathbf{F}_{k,l}^{(i)} = \left(\mathbf{H}_{k,l}^{eqH}\left(\mathbf{I}_p - \mathbf{R}_k^{(i-1)^2}\right)\mathbf{H}_{k,l}^{eq} + \mathbf{I}_p\sigma^2\right)^{-1}\mathbf{H}_{k,l}^{eqH}\boldsymbol{\Delta}_k^{(i)} \tag{4.19}$$

and

$$\mathbf{B}_{k,l}^{(i)} = \mathbf{H}_{k,l}^{eq}\mathbf{F}_{k,l}^{(i)} \tag{4.20}$$

d) MMSE equalizer

Considering MMSE at the first detection block we have the following feedforward and feedback matrices that were designed to take into account the residual aligned interference

$$\mathbf{F}_{k,l}^{(i)} = \left(\mathbf{H}_{eq,kk,l}^{H} \left(\mathbf{I}_P - \mathbf{R}_k^{(i-1)^2} \right) \mathbf{H}_{eq,kk,l} + \sum_{j=1, j\neq k}^{K} \mathbf{H}_{eq,kj,l}^{H} \mathbf{H}_{eq,kj,l} + \mathbf{I}_P \sigma^2 \right)^{-1} \mathbf{H}_{eq,kk,l}^{H} \Delta_{k,l} \qquad (4.21)$$

and

$$\mathbf{B}_{k,l}^{(i)} = \mathbf{H}_{eq,kk,l} \mathbf{F}_{k,l}^{(i)} \qquad (4.22)$$

For both equalizer cases $\Delta_k^{(i)}$ is defined as

$$\Delta_k^{(i)} = \left(\mathbf{I}_p - \mathbf{R}_k^{(i-1)^2} \right) - \frac{\lambda_k^{(i)}}{L} \mathbf{I}_p \qquad (4.23)$$

Where λ_k is the Lagrangian multiplier which is selected to ensure the constraint $\frac{1}{L} \sum_{l=0}^{L-1} \mathbf{tr}\left(\mathbf{F}_{k,l}^{(i)T} \mathbf{H}_{k,l}^{eqT} \right) = P$.

This residual aligned interference $\sum_{j=1, j\neq k}^{K} \mathbf{H}_{eq,kj,l}^{H} \mathbf{H}_{eq,kj,l}$ in (4.21) tends to zero when SNR tends to infinite and, thus the performance of ZF and MMSE tends to each other.

4.3. Results

In this section we present a set of performance results for the proposed scheme (joint IA ZF and IB-DFE). The considered scenario has *K*=3 (transmitter-receiver pairs) sharing the same resources. Also, we consider that each terminal is equipped with 2 and 4 antennas (*M*=2, 4). Note that for *M*=4, 2*L*-length data blocks are transmitted in parallel (*P*=2). The main parameters used in the simulations are based on LTE standard[9], and presented in Table 4.

It was, also, assumed there is perfect synchronization and channel estimation. The results are presented in terms of average BER as function of E_b / N_0.

The parameters of the LTE channel are:

Variable	Value
FFT size	1024
Sampling Frequency	15.36 Mhz
Useful Symbol Duration	66.67 μs
Cyclic prefix duration	5.21 μs
Overall Symbol Duration	71.88 μs
Sub-carrier Separation	15 Khz
Available Sub-Carriers	128
Modulation	QPSK

Table 4.1 LTE channel parameters.

1. **MIMO 2x2 and 4x4 uncorrelated Rayleigh channel**

In figures 4.4 and 4.5 is evaluated the performance between ZF and MMSE based equalizers as also MF curve for comparison in uncorrelated Rayleigh channels.

In Fig. 4.4 is presented the performance for 4 iterations with ZF based equalizer and we can observe that MMSE outperforms ZF even with 1 iteration as expected, since noise is enhanced namely in frequency deep notches. For a BER=$1.0e^{-3}$, ZF with 1 iteration has a penalty for MF of approximately 5 dB and 2 dB for the iteration 2.

In Fig 4.5 we can observe the performance of MMSE equalizer. For a BER=$1.0e^{-3}$, MMSE (IB-DFE with 1 iteration) has a penalty of 4 dB for MF and a penalty of 1 dB with 2 iterations.

In both figures, with the increase of iterations, the implemented scheme tends to MF but the gain between iteration is decreasing.

In figures 4.6 and 4.7 the same channel scenario was applied but the number of antennas was changed to a MIMO 4x4 scenario. The space-diversity order achievable is higher than for *M*=2. Therefore, the performance gain between the IA ZF/IA MMSE and IA ZF+IB-

DFE/IA MMSE+IB-DFE with four iterations is much higher than in the scenario with *M*=2, since this scheme is able to achieve the maximum diversity order even if the interference level is higher.

Note that for this scenario the IB-DFE based equalizer must deal with inter-block interference, since two length-128 blocks are transmitted simultaneously by each transmitter, and residual inter-carrier interference. Therefore, the proposed scheme is quite efficient to separate the spatial streams, even in the presence of residual inter-user interference, and achieve the higher diversity order inherent to this scenario, with only a few iterations.

In figure 4.6 ZF with 1 iteration has a penalty of 7 dB for MF and an improvement of 1 db for the MIMO 2x2 correspondent. For 2 iterations, ZF achieves a gain performance of approximately 2 dB in comparison of MIMO 2 x 2 systems. In figure 4.7 we observe a performance gain of approximately 1 dB for the first iteration in comparison with 2 x 2 environment and a 3 dB gain for the second iteration.

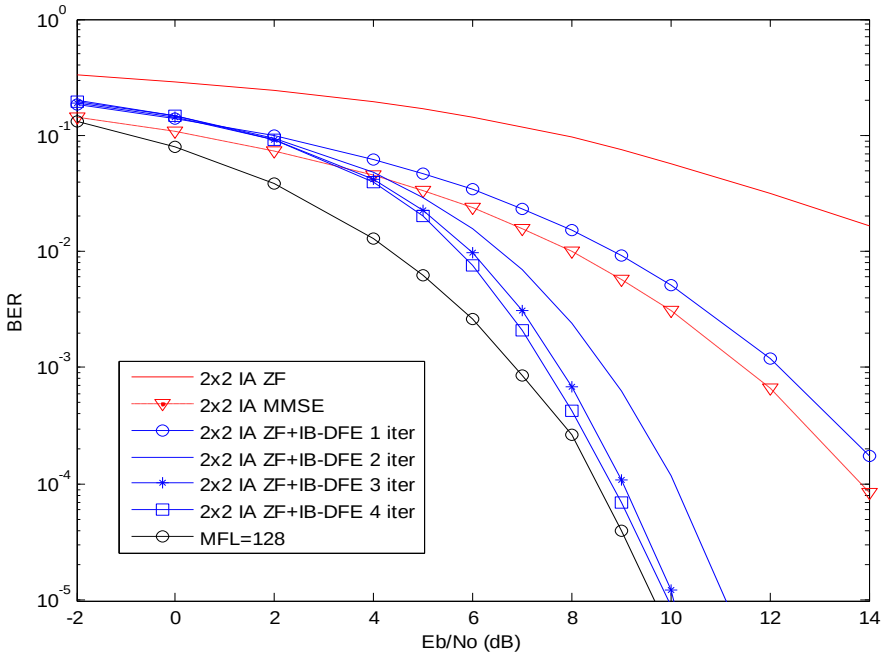

Fig. 4.4 Performance evaluation of the proposed scheme for ZF and M=2.

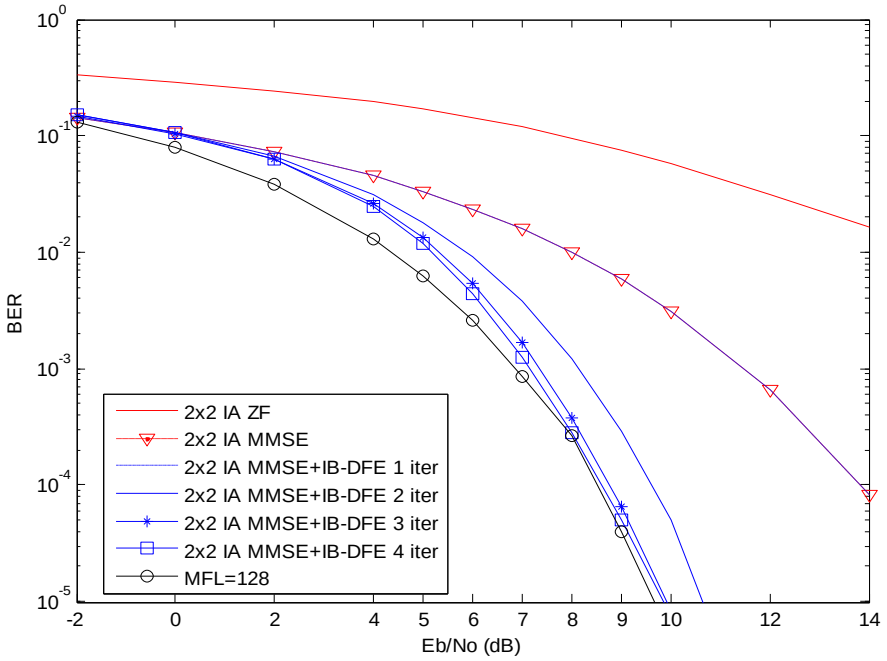

Fig. 4.5 Performance evaluation of the proposed scheme for MMSE equalizer and M=2.

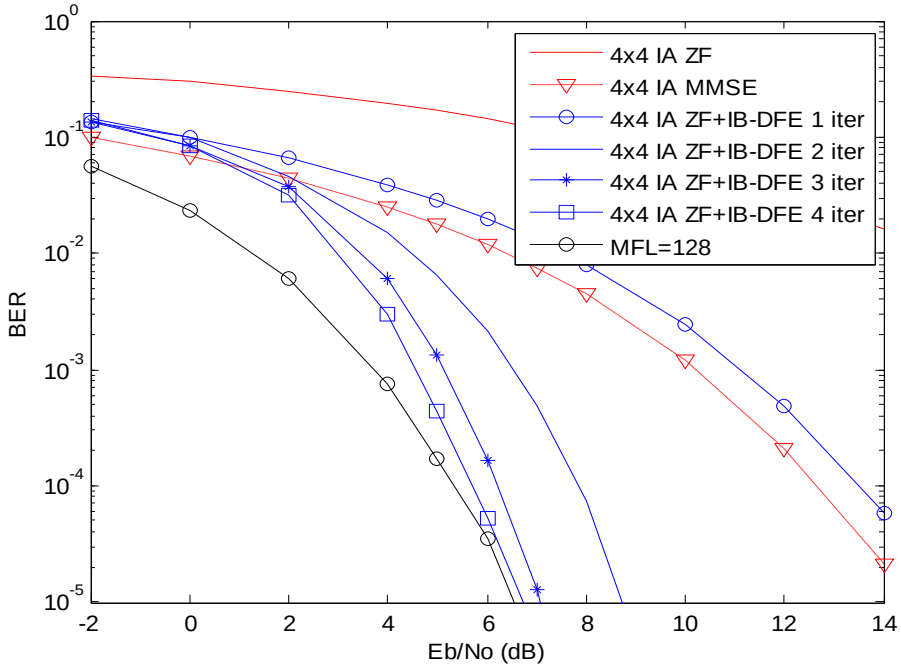

Fig. 4.6 Performance evaluation of the proposed scheme for ZF equalizer and M=4.

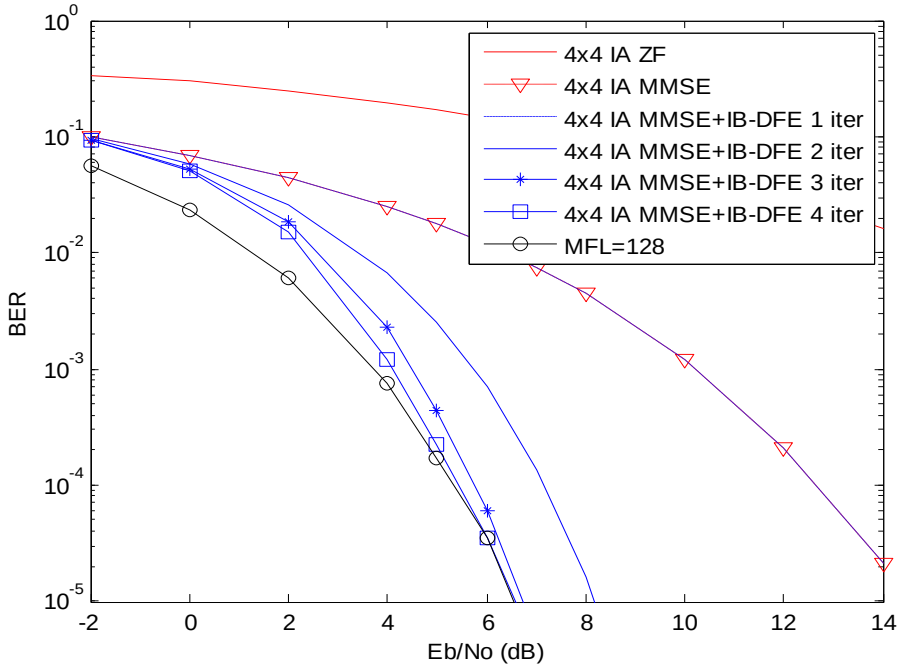

Fig. 4.7 Performance evaluation of the proposed scheme for MMSE equalizer and M=4.

2. **MIMO 2x2 and 4x4 LTE standard channel parameters**

In this scenario it was used a LTE extended typical urban channel model with 9 taps[9]. With these parameters and interleaved sub-carriers, there were obtained results that are depicted in figures 4.8 through 4.11 for the performance of this scheme in a LTE urban channel model. The conclusions are similar between the results of uncorrelated Rayleigh channel and LTE channel. For all LTE channel studied cases, the difference for a BER=$1.0e^{-3}$ between iterations is the same of the uncorrelated Rayleigh channel which indicates that the system has a similar response for the 2 studied channels. In *M*=2, the gap between uncorrelated Rayleigh channel and LTE can be noticed and it is approximately, for a BER=$1.0e^{-3}$, of 0.5 dB but when we have *M*=4, the gap decreases because we achieve maximum space-time diversity order on both cases which make the difference between them not significant.

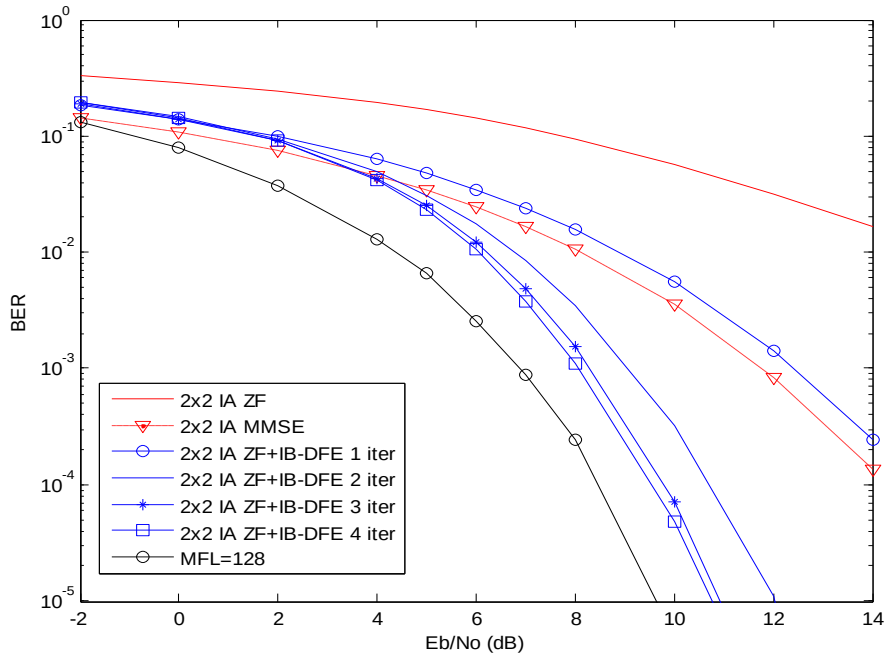

Fig. 4.8 Performance evaluation of the proposed scheme for ZF and M=2 on LTE standard channel.

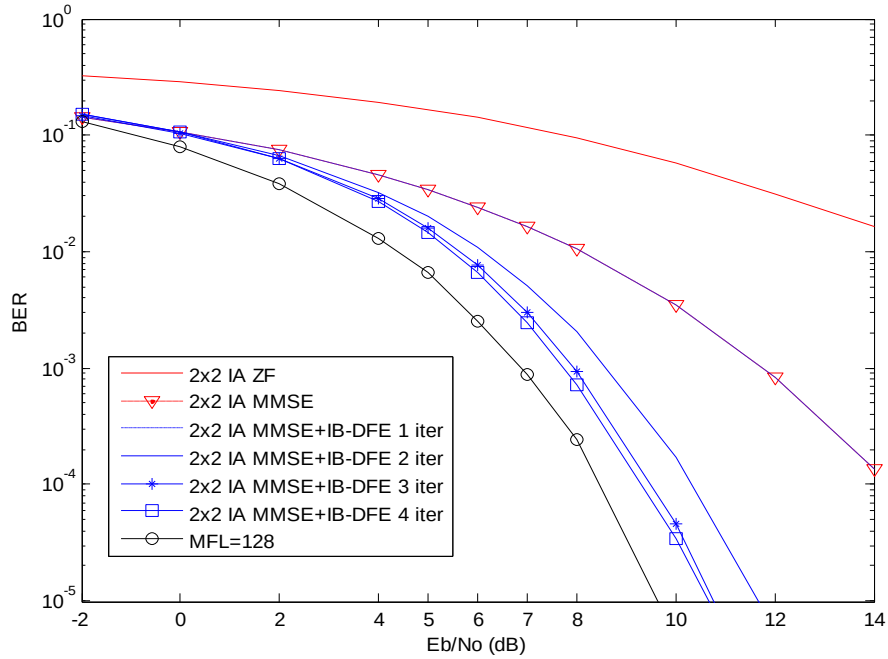

Fig. 4.9 Performance evaluation of the proposed scheme for MMSE and M=2 on LTE standard channel.

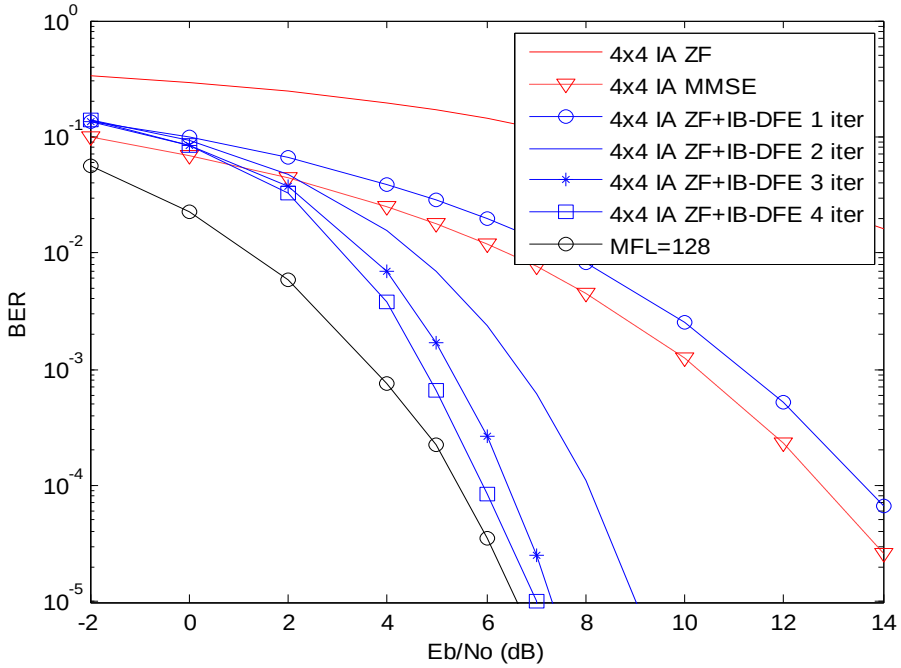

Fig. 4.10 Performance evaluation of the proposed scheme for ZF and M=4 on LTE standard channel.

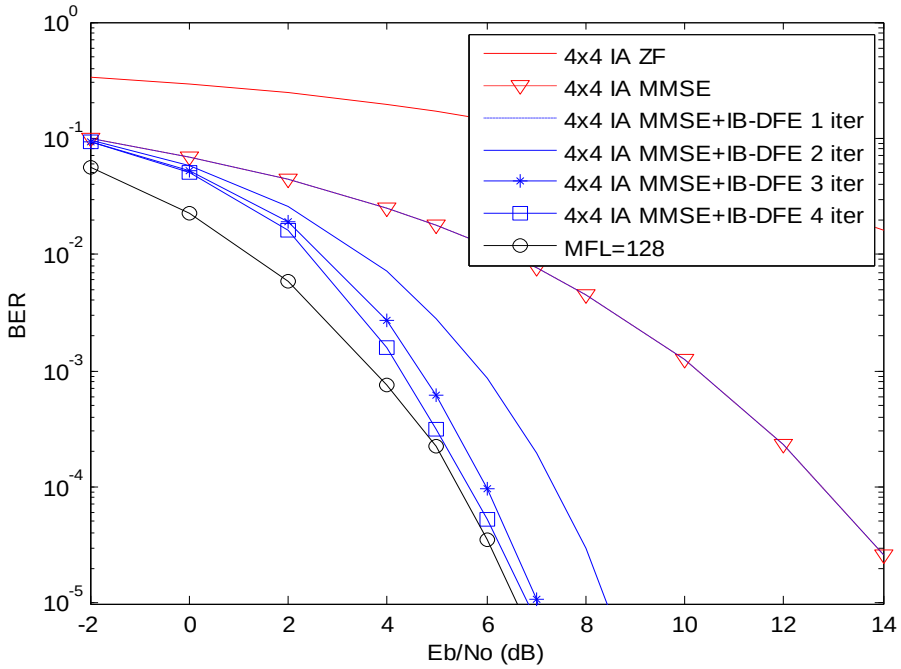

Fig. 4.11 Performance evaluation of the proposed scheme for MMSE and M=4 on LTE standard channel.

3. **Simulation with Channel Coding**

The results of the Fig. 4.12 and 4.13 were obtained for the IA MMSE+IB-DFE with MIMO 2x2 and 4x4, considering a half rate channel convolutional turbo code (CTC) specified for the LTE. We can observe a major improvement using CTC coding but the gain between iterations is lesser than when we did not have the referred coding. In figure 4.12 the gain between iterations is irrelevant and for a MIMO 4 x 4 system there is a gain of approximately of 0.5 dB for a BER=$1.0e^{-3}$.

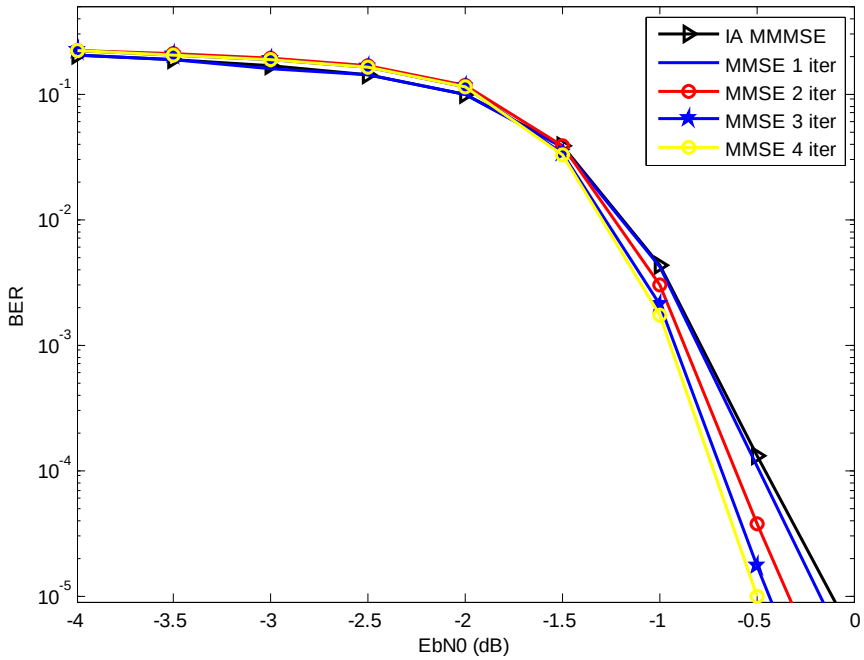

Fig. 4.12 Performance evaluation of the proposed scheme for MMSE and M=2 with channel coding

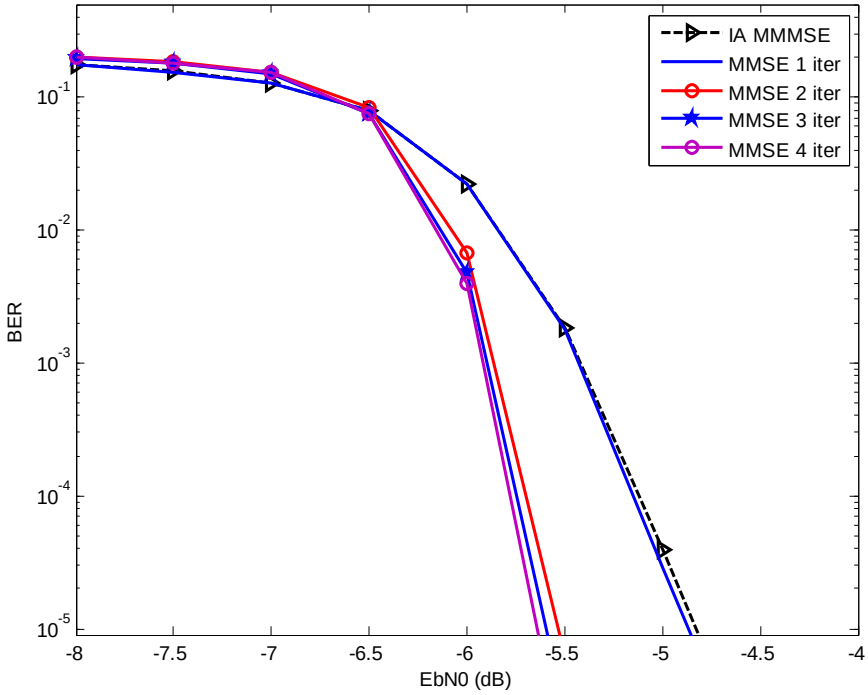

Fig. 4.13 Performance evaluation of the proposed scheme for MMSE and M=4 with channel coding

5. Conclusion

The increasing demand for wireless services has created the need for cost effective transmission techniques that can exploit scarce spectral resources efficiently. To achieve high bit rates, needed to meet the quality of service requirements of future multimedia applications, MC-CDMA has been considered as a candidate air-interface, especially for downlink. Conventional frequency domain equalization schemes employ a linear FDE optimized under the MMSE criterion. However, the residual interference levels might still be too high, leading to performance degradation. One interesting recent scheme to efficiently eliminate the interference and achieve a linear capacity scaling is IA. With this strategy more interferers can be completely cancelled than with other interference cancellation methods. Thus, in this thesis we efficiently combined interference alignment at the transmitter with frequency domain equalization at the receiver for MIMO MC-CDMA based systems.

In this thesis we started with a quick overview of the evolution of cellular communications. In the next chapter it was introduced the basic concepts of the systems that were used to accomplish this thesis as a general multi-carrier concept, namely OFDM concept and MC-CDMA and the introduction of Interference Alignment. In chapter 3, it is presented a deep view of MIMO technologies, the IB-DFE block and IA concept.

In chapter 4, it was presented the developed system where the two technologies discussed above, i.e., IA and IB-DFE concepts were combined. In first place, it was performed an IA-precoded at chip level and, secondly, the receiver was designed in two steps: first a ZF or MMSE based equalizer to remove users' aligned interference. Then and

after a white processing noise an IB-DFE based equalizer was designed to remove both the residual inter-user aligned and inter-carrier interference.

The developed simulation platform is flexible where we can configure several parameters as the number of antennas in base station and user, modulation, number of sub-carriers, etc.

The results have shown that the performance of the proposed scheme is close to the one of MF, with only a few iterations (2-4). Since the algorithm requires a reduced number of iterations the complexity is not significant and can be used in practical systems. Using a CTC channel coding we get major improvements in the performance of the proposed system.

To conclude we can clearly state that the proposed receiver structure is an excellent choice for the IA-precoded MC-CDMA based systems since the scheme achieves the maximum degrees of freedom (multiplex data symbols) provided by the IA precoding, while allowing a close-to-optimum space-diversity gain, with a performance close to the matched filter (MF).

5.1. Future Work

Some future work that can be done:

- In this work we used a closed form solution for 3 users. It would be interesting to extend to a system with more than 3 users.
- In this work we considered hard decisions in the feedback loop and it would be interesting to compare the performance considering soft decisions.
- It was assumed perfect channel information and synchronization and it would be of interest assess the algorithm under imperfect channel information.

Bibliography

[1] 4G Americas, "Mobile Market Shares by Technology," 2013. [Online]. Available: http://www.4gamericas.org/index.cfm?fuseaction=page&pageid=565. [Accessed: 15-Nov-2013].

[2] N. Narang and S. Kasera, *2G Mobile Networks*, 1st ed. Tata McGraw-Hill Education, 2006.

[3] C. K. Toh, *Ad Hoc Mobile Wireless Networks: Protocols and Systems*, 1st ed. Prentice Hall, 2001, p. 336.

[4] S. Kasera and N. Narang, *3G Networks*, 1st ed. Tata McGraw-Hill Education, 2004, p. 570.

[5] C. Cox, *An Introduction to LTE: LTE, LTE-Advanced, SAE and 4G Mobile Communications*, 1st ed. Wiley, 2012, p. 352.

[6] Motorola Inc., "4G Network Migration cdma2000™ to LTE Evolution White Paper." p. 8, 2009.

[7] WiMAX Forum, "Mobile WiMAX – Part I: A Technical Overview and Performance Evaluation." p. 53, 2006.

[8] Tran et al, "Overview of enabling technologies for 3GPP LTE-advanced," *EURASIP J. Wirel. Commun. Netw.*, no. 2012:54, 2012.

[9] 3rd Generation Partnership Project, "Overview of the 3GPP Long Term Evolution Physical Layer." 3. 3GPP TS 36.201 V8.1, 2007.

[10] 4G Americas, "Global HSPA-LTE Forecast," 2013. [Online]. Available: http://www.4gamericas.org/index.cfm?fuseaction=page&pageid=1940. [Accessed: 15-Nov-2013].

[11] E. L. Pinto and C. P. de Albuquerque, "A técnica de transmissão OFDM," *Telecomunicações*, vol. 05, no. 1, 2002.

[12] S. Hara and R. Prasad, "Overview of multicarrier CDMA," *IEEE Commun. Mag.*, vol. 35, no. 12, pp. 126–133.

[13] M. Munster, L. Hanzo, B. J. Choi, and T. Keller, *OFDM and MC-CDMA for Broadcasting Multi-User Communications, WLANs and Broadcasting*. John Wiley & Sons, Inc.

[14] Z. Wu and C. R. Nassar, "FD-MC-CDMA: A Frequency-Based Multiple Access Architecture for High Performance Wireless Communication," *IEEE Trans. Veh. Technol. VOL. 54, NO. 4, JULY 2005*.

[15] E. M. D. Conde, "Detection Techniques for the uplink in LTE," Universidade de Aveiro, 2012.

[16] V. Cadambe and S. Jafar, “Interference alignment and degrees of freedom of the k-user interference channel,” *IEE Trans. Inf. Theory*, vol. 54, no. 8, pp. 3425–3441.

[17] S. A. Jafar, “Interference Alignment — A New Look at Signal Dimensions in a Communication Network,” *Foundations and Trends® in Communications and Information Theory*, vol. 7. pp. 1–134, 2010.

[18] K. Fazel and S. Kaiser, *Multi-Carrier and Spread Spectrum Systems*, 1st ed. New York: John Wiley & Sons, Inc, 2003, p. 320.

[19] A. Gameiro and A. Silva, “Transmission Strategies for MISO Downlink MC-CDMA Mobile Systems,” *Wirel. Pers. Commun*, vol. 54, no. 3, pp. 521–541.

[20] D. Falconer, S. Ariyavisitakul, A. Benyamin-Seeyar, and B. Eidson, “Frequency Domain Equalization for Single-Carrier Broadband Wireless Systems,” *IEEE Commun. Mag.*, vol. 40, no. 4, pp. 58–66.

[21] 3G Americas, “MIMO Transmission Schemes for LTE and HSPA Networks.” 2009.

[22] F. C. Ribeiro, “Multicell Cooperation for Future Wireless Systems,” ISCTE - Instituto Universitário de Lisboa, 2012.

[23] S. W. Peters, “Cooperative algorithms for MIMO interference channels,” *Heath Jr. , R.W.*, vol. 60, no. 1, pp. 206–218, 2011.